Schweizerische Eidgenossenschaft
Confédération suisse
Confederazione Svizzera
Confederaziun svizra

Département fédéral de l'environnement,
des transports, de l'énergie et de la communication DETEC

Office fédéral de l'énergie OFEN
Recherche énergétique

Intermediate report 14.12.2018

Project VITES

Vacuum Insulated Thermal Energy Storage

Date : 14.12.2018

Lieu : Berne

Mandant :
Office fédéral de l'énergie OFEN
Programme de recherche XY
CH-3003 Berne
www.ofen.admin.ch
energieforschung@bfe.admin.ch

Cofinancement :
Laboratoire d'énergétique solaire et de physique de bâtiment (LESBAT)
CH-1401 Yverdon-les-Bains
www.heig-vd.ch

Mandataires :
HEIG-VD
Laboratoire d'énergétique solaire et de physique de bâtiment (LESBAT)
Av. des Sports 20, CP 521
CH-1401 Yverdon-les-Bains
www.heig-vd.ch

Auteurs :

Vittorio Palmieri	palmieri@tvpsolar.com
Sara Eicher, HEIG-VD	sara.eicher@heig-vd.ch
Martin Guillaume, HEIG-VD	martin.guillaume@heig-vd.ch
Jacques Bony, HEIG-VD	jacques.bony@heig-vd.ch
Stéphane Citherlet, HEIG-VD	stephane.citherlet@heig-vd.ch
Philippe Bonhôte, HEIG-VD	philippe.bonhote@heig-vd.ch

Responsable de domaine OFEN :	Stefan Oberholzer, stefan.oberholzer@bfe.admin.ch
Chef de programme de l'OFEN :	Stefan Oberholzer, stefan.oberholzer@bfe.admin.ch
Numéro du contrat de l'OFEN :	SI/501690-01

Responsable de domaine OFEN :	Elimar Frank, elimar.frank@frank-energy.ch
Chef de programme de l'OFEN :	Elimar Frank, elimar.frank@frank-energy.ch
Numéro du contrat de l'OFEN :	SI/501691-01

Résumé

Le but de ce projet est d’analyser le concept d’un accumulateur de stockage thermique à double paroi avec du vide poussé entre les deux parois afin de réduire de manière considérable les pertes thermiques. Les principales applications visées par ce produit sont les installations solaires thermiques intégrées aux procédés de chaleur industrielle, mais il peut également servir pour des applications résidentielles et avec d’autres sources d’énergie.

Pour mener à bien cette étude, les activités suivantes ont été réalisées en 2018 :

- recherche bibliographique sur l'état de l'art des systèmes TES, études et applications
- analyse structurelle du concept VITES
- analyse thermique préliminaire du concept VITES
- participation à l'annexe 30 et à l’IEA Tâche 58/annexe 33 de l'AIE

Summary

This project aims to analyse the concept of a high performance, double-wall vacuum insulated thermal storage container in order to significantly reduce heat losses. The main applications for this product are solar thermal systems integrated into heating processes, but it can also be used for residential applications and with other energy sources.

In order to carry out this study, the following activities were performed in 2018:

- literature review of the state of the art of TES systems and review of existing research on vacuum insulated container technology and applications
- structural analysis of the designed VITES concept
- preliminary thermal analysis of the VITES concept
- participation to ECES Annex 30 and IEA Task 58/Annex 33

Table of Contents

Abbreviation list

AISI	American Iron and Steel Institute
ECES	Energy Conservation and Energy Storage
FEA	Finite Element Analysis
OFEN	Office fédéral de l’énergie
SHC	Solar Heating and Cooling
TES	Thermal energy storage

1 Introduction

The Swiss Energy Strategy 2050 sets an approach to reach a sustainable energy supply in Switzerland by 2050. In addition to the phase-out of nuclear power, the strategic objectives include measures to increase the use of renewable energy and the energy efficiency of buildings, mobility, industry and appliances [1]. However, most renewable energy sources are intermittent in nature so that energy production is not in phase with energy demand. Energy storage has, therefore, become an important research topic and the development of efficient, inexpensive energy storage systems as important as the quest for new energy sources [2].

Thermal energy accounts for some 75% of the final energy consumption in Switzerland. More than 50% of this energy is used for space heating, domestic hot water production and industrial process heating [3]. In these applications, full use of renewable energy can only be achieved by providing adequate energy storage options. Therefore, thermal energy storage (TES) could play a major role in global energy efficiency improvement by increasing the share of renewable energy production and of waste heat recovery. In addition, the Federal Energy Research Masterplan [4] considers decentralised heat and cold storage as one of the research area to be focused by 2020. Still, for a better market penetration, major challenges need to be overcome not only on the technical side (long-term capacity, longer lifetime, higher efficiency, improved safety) but also on the financial side with better return on investment.

In recent years, some developments have been made regarding insulation of TES. Double-wall vacuum insulated systems for sensible heat storage, using low levels of vacuum and gap filling materials to increase thermal resistance, are one of them.

The goal of this project is to develop the concept of a high performance, double-wall hot water thermal storage container with high vacuum and no filling material in the gap between the walls to decrease heat losses. Such a device must have an acceptable cost and should be of interest to solar thermal industrial and residential systems as well as to store thermal energy from any other energy source.

This research in line with the Swiss Energy Strategy 2050 through:

- Valorisation of solar heat and other renewable energies
- Improvement of the performance of sensible TES
- Improvement of energy efficiency in buildings and industrial processes
- Reduction of environmental impacts

Participation to the Annex 30: Thermal Energy Storage for Cost-effective Energy Management and CO_2 Mitigation [5], have not only allowed to deeper the knowledge of this topic but also to evaluate current challenges in the development of TES, some of them addressed in this project.

Beginning 2017 a joint SHC Task 58/ECES Annex 33 entitled Material and Component Development for Thermal Energy Storage [6] was launched dealing with advanced materials for latent and chemical storage. Although the focus in on materials, the current project for which the development of a novel TES concept is aimed, fits well with the overall work developed in this joint task/annex.

2 Project aim

The aim of this project is to develop a high performance, double-wall vacuum insulated hot water thermal storage container. In this concept, for which a high vacuum level (less than 0.001mbar) is foreseen, losses by convection and conduction should tend towards zero. The main heat losses of the tank being limited to radiation and to the thermal bridges present in the wall of the tank and fittings. In addition, this new container will have to be competitive from a financial point of view compared to standard insulated containers on the market. To achieve this goal, several parameters will be investigated, in particular:

- structural analysis of the VITES concept
- the optimisation between the level of vacuum achieved, the performance and cost
- the need to use reflective surfaces
- the need to minimise thermal bridges
- the behaviour of the container according to the hydraulic connections.

Target applications for this device would be in the industrial sector, as temperature levels are normally higher than in building applications so that storing energy losses are equally larger. In addition, temperatures over 100 °C prevents the use of polyurethane foam as insulating material, which greatly increases insulation costs. However, this project will also tackle the individual and collective housing market because the energy saving potential of this technology appears to be significant even at lower temperatures as the potential market is significantly higher. All these developments are in line with the strategy of meeting industry demands with the expertise of TVP Solar.

In terms of investment cost, the goal of this project is to design a storage device that does not exceed the maximum acceptable storage capacity cost (SCC_{acc}) as defined in the IEA SHC Task 42 / ECES Annex 29 [7], see Figure 1. Thus, for a solar thermal application in the building sector the cost of the TES should not exceed 300€/kWh_{cap} (€ per kWh of installed storage capacity), while for the industry sector, acceptable prices should be below 100€/kWh_{cap} for a process that needs several cycles per day.

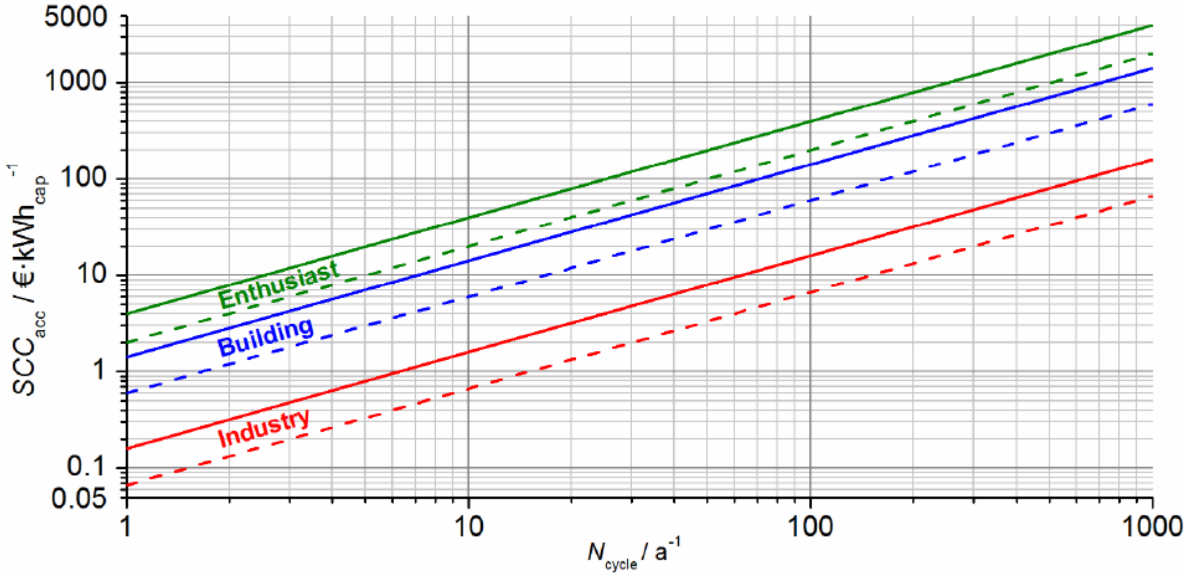

Figure 1: Maximum acceptable storage capacity costs SCC_{acc} for three user classes as a function of storage cycles per year Ncycle; enthusiast high/low case (green solid/dashed line), building high/low case (blue solid/dashed line), and industry high/low case (red solid/dashed line) [7].

To develop a sound vacuum insulated storage container, this project will make use of the renowned and comprehensive experience of TVP Solar, experts on thermal vacuum power charged technology and industrial partner of this project.

It has been estimated to about 1.4 million GWh/year, the potential savings from a wider use of hot and cold storage systems in the industrial and domestic sectors in Europe [8]. Within the Swiss context, the estimated value is about 4500 GWh/year in the building sector alone. The use of TES for industrial waste heat recovery is also of great importance with a 5.3 TWh of waste heat estimated in the Swiss industry [9].

2.1 Project steps

The project is divided into 3 work packages:

- WP1: Concept development
- WP2: System integration
- WP3: Dissemination

In order to successfully develop the VITES storage device, the following objectives have been defined:

- literature review of existing concepts, products and research in the field of TES, particularly for hot water thermal storage
- structural analysis of the VITES container to validate the proposed design, ensure conformity to the target applications and assess the impact of changing conditions
- thermal design analysis to assess the heat transmission process, temperature distributions and the influence of several parameters on the overall thermal behaviour of the VITES container
- numerical simulation of the annual performances of the VITES container under different conditions and for different applications and assessment of potential gains

3 Literature review

3.1 Thermal energy storage (TES)

Thermal energy storage is defined as the temporary storage of thermal energy at high or low temperature levels. These systems are required when the heat demand is not in phase with heat production. Of great importance in many engineering fields, they are particularly used in buildings for short-term storage of domestic hot water and industrial processes. However, long-term storage is also possible but imply larger storage containers to harvest large quantities of energy, such as waste heat from industrial processes, to use, for example, in large-scale central heating systems.

The technology offers, in this way, the possibility to offset the mismatch between demand and availability of thermal energy by collecting and storing energy for use at a later time. Primarily designed to store solar energy, these systems can also be employed to store any other timely-based energy source such as waste heat for which availability and utilisation periods differ.

The advantages of a well design TES system can be summarised as follows:

- improved energy efficiency
- increased reliability of the required supplied energy
- reduced investment and maintenance costs
- reduced environmental impacts

According to the storage mechanism, TES can be classified into:

- sensible heat storage: by heating or cooling a liquid or a solid storage medium
- latent heat storage: by the phase change of the storage medium (melts and vapour)
- thermochemical heat storage: by thermochemical reactions

Storage of heat has been traditionally in the form of sensible heat with water as the most common storage medium. Latent heat storage as become an important research topic in the last decade due to its operational advantages of smaller storage containers and small temperature variations. This review will concentrate on sensible heat storage for water heating applications.

A key aspect of TES systems is the insulation of the tank to reduce heat losses. The state of the art for thermal storages is conventional building insulation materials such as mineral wool, expanded polystyrene and polyurethane foam [10]. Improving the current insulation factor of these materials is difficult because of their high thermal conductivities and large insulation thicknesses. Therefore, advanced insulation materials have been developed and tested in real case studies, see for example [11,12].

The open literature indicates an important research and development activity taking place in Europe particularly for vacuum insulated TES. The availability of some commercial products based on this technology is also acknowledged in different case studies.

3.2 Sensible heat storage technologies

The most common material used in sensible heat storage is water as it has a high specific heat capacity and is cheap in comparison to any other storage medium. At low temperature, water is one of the best storage medium and the most widely used for solar water heating applications. Due to the boiling point constraint of water, high temperature applications require increasing the system pressure [13]. Research have shown that water tank storage is a cost-effective option but with room for improvement in terms of internal stratification temperatures and thermal insulation [14]. For this latter, research is now focus on evacuated super-insulation materials with much lower effective thermals conductivities and with no moisture deterioration, as is the case in the most common insulation materials [15].

Underground storage of sensible heat is typically used in large-scale applications and is well suited for seasonal storage, i.e. using summer season stored heat in the heating season. According to a recent review [16], TES systems based on sensible heat storage have storage efficiencies between 50 to 90% depending on the storage medium and insulation technology. In general, sensible heat storages are simpler in design than latent or thermochemical storages but are bigger in size.

3.3 Vacuum insulated materials

Super insulating materials have been used in the past to insulate passive houses. [17] reported a building related application with the integration of vacuum insulation into different building elements.

Vacuum insulation panels and aerogel based products have 6 to 10 times lower thermal conductivity [18] and, consequently, lower insulation thickness when compared to traditional insulating materials. They offer a suitable option for insulating TES.
The characterisation of the effective thermal conductivity of the most widely proposed nanostructured insulants, such as expanded perlites and fumed silica, under different operating conditions lead to a number of publications [12,15,19,20]. Results demonstrate that super insulating materials are best for TES with certain dimensions and for large TES these materials are less effective and not economical. The study [12] demonstrated that vacuum insulation with perlite is an appropriate and economic method for high temperature (up to 300 °C) since effective thermal conductivities remain low.

3.1 Vacuum insulated TES: research and market

The potential of vacuum insulation materials for different hot water storage sizes and operating temperatures has also been addressed in the open literature.

The use of concrete long-term hot water thermal storage of 100 m^3 with vacuum insulated panels (fumed silica) have shown a 90% reduction in emissions and 80% in storage losses [11]. The project also shows that additional costs for the TES are covered by the energy savings.

Another storage concept was developed and tested for hot water applications [18]. The 15.5 m^3 evacuated double vessel filled with pearlite and containing water at 86 °C presented an overall cooling rate of 0.23K/day including thermal bridges.

This development led to a commercialised German product capable to ensure long-term operation without considerable heat losses [21]. Manufacturing the tank is indicated to be a major issue because it requires precise welding and leaks inspection. The evacuation process also takes long. The price of a 10 to 15 m^3 vacuum storage is indicated to range from EUR 20’000 to 25’000. From 35 m^3 on, the price of a vacuum TES and a conventional tank are reported to be the same.

Within the framework of a research project financed by OFEN (COLAS) [22], the LESBAT had the opportunity to measure the performance of two TES tanks in an industrial application for bitumen storage. It was observed that the 40 years old thermal insulation in place was no longer effective, which lead the industrial partner to replace them. Despite this measure, one of the new TES tanks presented heat losses up to 10 times higher than the expected theoretical value for this type and thickness of insulation. In some cases, heat losses could represent 15 to 40% of energy consumption like in the COLAS project [23]. The reason for this problem was the permeability of mineral wool to air and the effect of moisture on the air conductivity. This case highlights the importance of using insulation that is not affected by moisture or aging, such as in a vacuum TES.

In Switzerland, efforts are currently made to develop high temperature TES relevant to industrial applications such as the case of VITES. [24] made a comprehensive analysis of the potential of integration of vacuum insulated TES in Swiss industries and found that 70% could profit from this technology. It has also been identified that replacing existing TES insulation is not possible with vacuum insulation.

Research is also focusing on seasonal TES of low temperature for building applications: space heating, domestic hot water and industrial processes [25]. Seasonal storage is a fundamental domain of action to meet the Energy Strategy 2050 objectives.

From these findings and constraints, the development of a new vacuum insulated TES is needed to reduce thermal losses at an affordable cost in order to meet Swiss energy engagements.

4 VITES design conception

The VITES concept is a vacuum insulated hot water heat storage that can be charged with solar energy or any other renewable energy and even waste heat. Its functional principle is to store heat in the form of temperature-layered hot water over long periods.

By definition, vacuum (space devoid of matter) is often considered to be the best known insulator. In fact, the lack of matter greatly minimises heat losses by conduction and convention and only radiation can occur. In the VITES concept, the vacuum insulation is obtained in the gap between the two concentric metal cylinders that form the container.

The VITES target design specifications are presented in Table 1.

Purpose	**Heat storage**
Container volume	Up to 3 m^3 (reference 0.8 m^3)
Storage medium	Water
Storage medium temperature	Up to 180 °C (reference 160 °C)
Storage medium pressure	Up to 16 bar
Container material	AISI 316L
Insulated material	Vacuum
Vacuum level	Less than 0.001 mbar
Vacuum insulation conductivity	0.01 W/m K
IR surface coating material of outer wall of inner tank	copper
Global heat loss coefficient	0.03 W/m^2 K
Design cost	Up to 300 €/kWh (building sector) Up to 100 €/kWh (industrial sector)

Table 1: Target design specifications of the VITES concept

4.1 Structural analysis

Because of the design operating pressures: up to 16 bar inside the container, less than 0.001 mbar in the double-wall gap and atmospheric pressure at the outside, the structural assessment of the proposed design was performed. The geometry and the structural analysis of the VITES concept is presented here.

VITES consists of two concentric stainless steel cylindrical tanks with hemispherical end caps. The inner tank contains pressurised hot water. The outer tank must withstand the vacuum between the two cylindrical shells to isolate the inner tank and minimise the heat exchange between the water and the outside ambient conditions.

For the structural analysis, the following characteristics are considered:

- Container capacity : 1 m^3
- Minimised heat exchange
- Four pipes for water circulation
- Attachment points on the top of the tank
- Minimised gap between the two cylindrical shells

The Final Element Analysis (FEA) of the VITES concept was performed with ANSYS [26]. It aimed to verify the total integrity of the chosen wall thicknesses and the buckling safety.

Two design prototypes were considered with characteristics differing in the supporting feet and thicknesses of the concentric tanks. The main geometrical dimensions of prototypes 1 and 2 are provided in Table 2.

Length	**2127 mm**
Outer shell external diameter	1000 mm
Inner shell external diameter	8000 mm
Inner shell thickness: cylindrical body	Prototype 1=8 mm; Prototype 2=5 mm
Inner shell thickness: hemispherical end caps	Prototype 1=8 mm; Prototype 2=12 mm
Outer shell thickness (cylindrical and hemispherical ends)	3 mm
Number of reinforcement C rings	3
Number of supporting feet	4

Table 2 : Main geometrical dimensions of prototypes 1 and 2

4.1.1 Material properties and allowable stresses

The material proposed for the VITES concept is a AISI 316L stainless steel. This molybdenum bearing austenitic stainless steel is commonly used for vacuum applications as it shows enhanced corrosion resistance and ductability [27]. The mechanical properties of this stainless steel are given in Table 3 [28].

Material	**AISI 316L**
Young's modulus	210 GPa
Poisson's ratio	0.3
Density	8000 kg/m^3
Elastic limit	205 MPa
Ultimate tensile strength	515 MPa

Table 3: Material properties used for the VITES concept [28]

4.1.2 Design of prototype 1

Figure 2 shows the design of prototype 1.

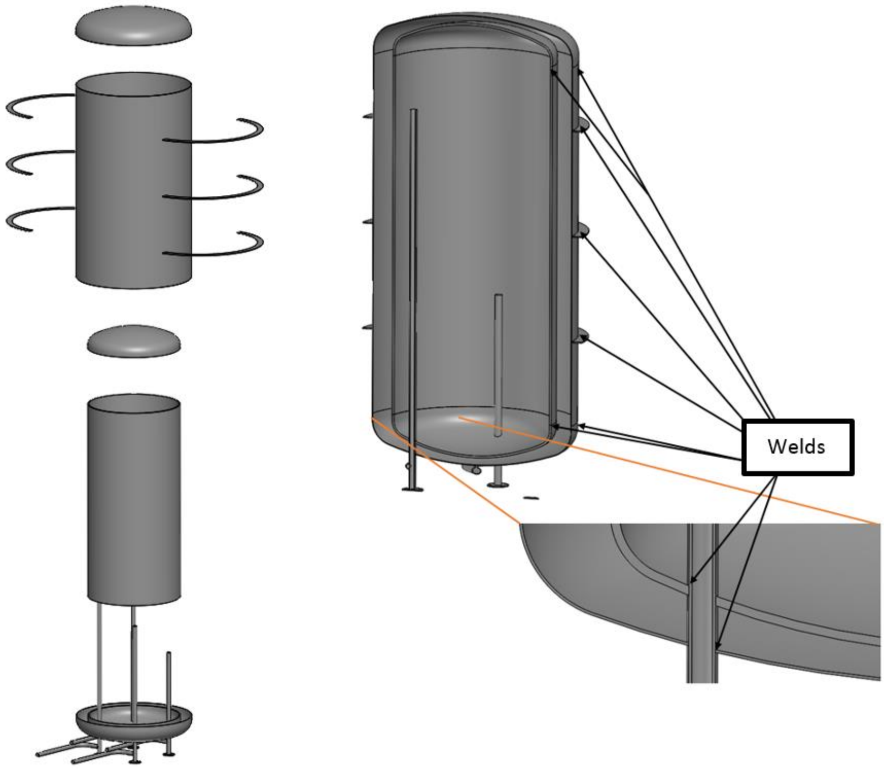

Figure 2 : Overview of prototype 1

The outer tank is reinforced with C shape rings to resist buckling caused by the vacuum between the two tanks. The inner tank is supported by four tubes welded to the hemispherical bottom end.

4.1.3 Design prototype 2

Figure 3 shows the design of prototype 2.

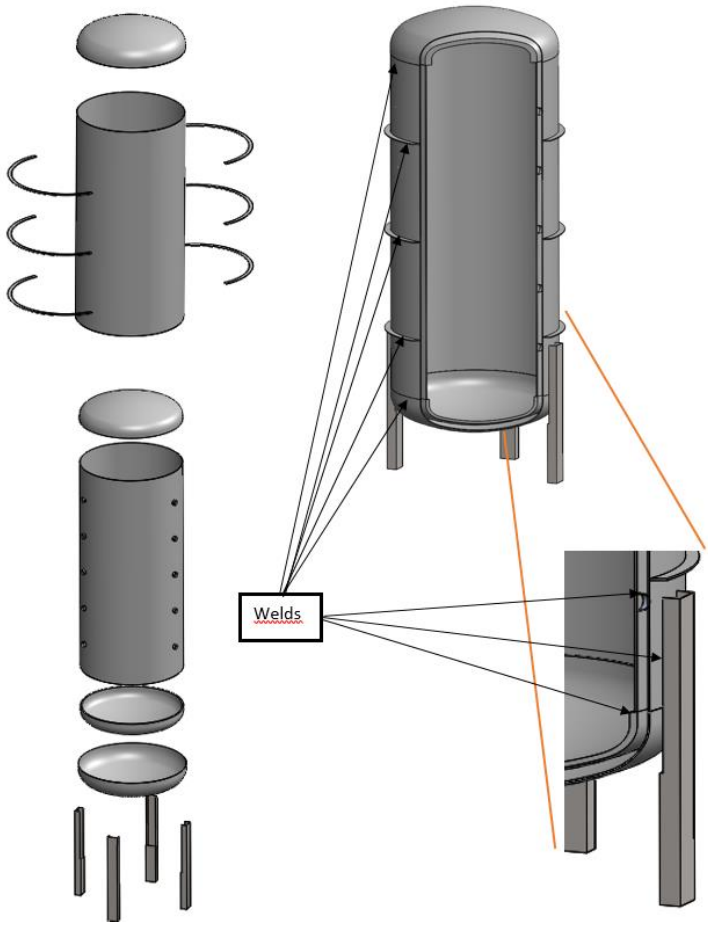

Figure 3 : Overview of prototype 2

The outer tank is also reinforced with C shape rings to resist buckling caused by the vacuum between the two tanks. The inner tank is supported by spacers welded at the inner side of the outer tank and the outer side of inner tank but not on the hemispherical end caps. The supporting feet are welded at the outer side of the outer tank cylindrical body.

4.1.4 FEA results

The main results of the structural analysis are provided in Table 4.

	Prototype 1	Prototype 2
Mass, kg	655	462
Global stress of inner tank, MPa	300	192
[1]Membrane stress of inner tank, MPa	190	134
Buckling (load multiplication)	6.2	9.6

Table 4 : Comparison of the structural analysis results for prototypes 1 and 2

Simulations show that prototype 2 with improved wall thicknesses presents lower constraints, in addition to a reduced overall mass when compared to prototype 1. A buckling analysis was also performed to check the stability (collapsing of the VITES container) of the prototype designs. Prototype 2 presents a buckling load 9,6 times higher than the nominal load and 1.5 times higher than prototype 1. Under these conditions no risk of buckling is foreseen. Given the results, prototype 2 is structurally acceptable and is retained for the remaining part of this project.

Please refer to Appendix 1 for further details of the FEA results.

4.2 Preliminary thermal analysis

4.2.1 Radiation heat transfer – Emissivity impact

As previously mentioned, vacuum insulation reduces dramatically the heat transfer by conduction and convention with no effect on the radiation transfer that becomes the predominate heat exchange mode, which depends on the emissivity of the walls and their temperatures. In order to anticipate the thermal simulations with ANSYS software, a preliminary thermal loss calculation for the radiation component was performed to investigate the effect of emissivity coating in the heat losses of the VITES concept.

For this calculation the VITES container is assumed to be a closed cylinder with flat ends instead of hemispherical end caps. Wall emissivity for the two concentric tanks was assumed to be 0.03 [29], a value easily achieved with a copper based coating on the evacuated side surfaces of the gap between the cylinders, to reduce the net radiation transfer.

Thus, two calculations are performed: one for the cylindrical body of the tank and the other for the upper and lower flat ends of the tank. The theoretical heat losses of the VITES container can be calculated as the net radiation exchange between the two flat plates added to that between the two concentric cylinders as given by [30]:

For flat plates:

$$q_p = \frac{A_p \sigma (T_1^4 - T_2^4)}{\frac{1}{\varepsilon_1} + \frac{1}{\varepsilon_2} - 1}$$

[1] Stress along the thickness of the shell

For concentric cylinders:

$$q_c = \frac{A_1 \sigma (T_1^4 - T_2^4)}{\frac{1}{\varepsilon_1} + \frac{1-\varepsilon_2}{\varepsilon_2}\left(\frac{r_1}{r_2}\right)}$$

With :

- q : specific heat transfer [W/m²]
- A_p : flat plate area (top and bottom) – mean value between diameter of inner and outer tank [m²]
- A_1: inner cylinder surface area [m²]
- σ : Stefan-Boltzmann constant 5,67.10^{-8} [W/m²/K⁴]
- ε_1, ε_2 : Emissivity of surface 1 (inner tank) and 2 (outer tank) [-]
- T_1, T_2 : surface temperature 1 (inner tank) and 2 (outer tank) [K]

This result was compared to the case where the VITES container is insulated with a conventional mineral wool material having a thermal conductivity of 0.06 W/m K to account for the humidity of the air [29]. The convection heat losses were estimated for a natural convection heat transfer coefficient of 10 W/m²K. Ambient temperature was taken at 20 °C.

The results are illustrated in Figure 4 for two emissivity values of the outer wall of the inner tank.

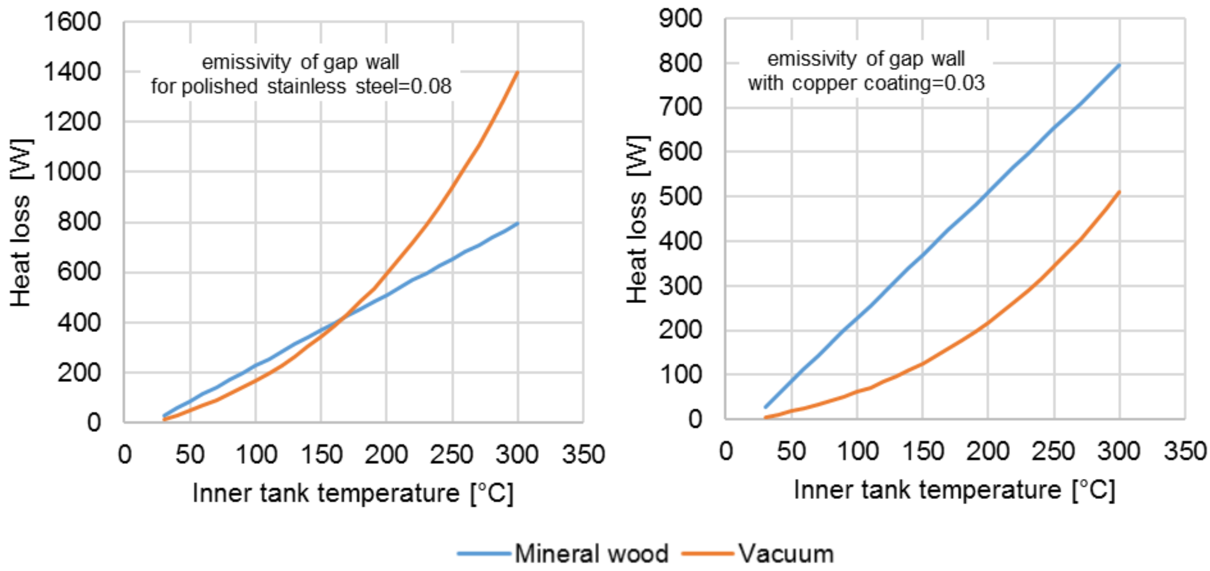

Figure 4 : Comparison of the heat loss rate between the VITES concept and an equivalent conventional insulated storage tank for two emissivity values

As expected, the higher the temperature difference between the inner tank and the ambient conditions, the higher the heat loss to the outside. Vacuum insulation is also seen to be more effective in preventing heat losses particularly at high temperatures where the low emissivity coating is able to significantly reduce the radiative thermal transport to values below those of conventional conduction losses. In addition, usual insulation materials such as mineral wool can be affected by moisture that heavily deteriorates their insulation properties due to an increase in the thermal conductivity.

For the reference operating temperature of 160 °C (see Table 1), heat loss is estimated to be nearly three times lower when using vacuum insulation with a low emissivity coating when compared to conventional insulation materials. This demonstrates that a low emissivity coating in the evacuated gap offers a tremendous advantage in the development of long-term sensible heat storages.

4.2.2 Conduction heat transfer – Spacers and water piping heat loss results

In prototype 2, spacers are used to maintain the space and properly position the two cylindrical concentric tanks. Spacers are available in a variety of shapes and materials to meet the particular needs of different applications. For this case, the choice of a proper spacer was defined by performing a conduction heat loss calculation in order to evaluate thermal bridges and minimise their impact. Based on previous experience, two materials: borosilicate and stainless steel were considered for the spacers as well as round and spring shapes. Heat losses in the water piping system was also calculated to evaluate the impact of thermal bridging and provide solutions to minimise it.

According to Figure 4 the overall radiation heat loss of the VITES concept, with applied copper coating, at the reference operating temperature of 160 °C is about 140 W. Table 5 presents the results of the conduction heat losses in the spacers and water piping under these conditions.

	Water piping		Spacers type		
			spring	round	
	Material				
	Stainless steel	Water	Stainless steel	Stainless steel	Borosilicate
Conductivity, W/m K	15	0.688	15	15	1
Length, m	0.100	0.100	0.150	0.030	0.030
External diameter, m	0.034	0.027	0.003	0.003	0.015
Internal diameter, m	0.027				0.010
Conduction surface area , m²	0.000	0.001	0.000	0.000	0.000
Coefficient, W/K	0.047	0.004	0.001	0.004	0.004
Conduction heat transfer, W	6.53	0.56	0.10	0.49	0.55
Number of elements	4	4	15	15	15
Total conduction heat transfer, W	26.1	2.2	1.5	7.4	8.2

Table 5 : Comparison of the conduction heat losses from spacers and water piping for different geometries and materials

The calculation indicates that the use of borosilicate spacers with low thermal expansion and high surface strength is not advantageous, presenting a similar conduction loss to stainless steel spacers. The use of spring spacers although presenting much lower conduction losses are also discarded because in comparison with the overall heat loss of the VITES concept, round spacers losses are still negligible and probably easier to manufacture. A 10 cm water piping seems also adequate as the conduction heat losses amount to less than 20% of the overall losses of the tank. Given these results, it is likely that round stainless steel spacers and water piping of 10 cm long will be adopted on the final VITES design, but at this stage, a decision has not yet been made.

5 Conclusions and perspectives

A literature review was conducted to provide a state of the art of TES systems and review the existing research on vacuum insulated container technology and applications. Few studies on double wall evacuated tanks were found and none employed a completely evacuated gap as designed in VITES.

The design concept was evaluated from the structural and thermal point of view. One of two prototypes was found to be structurally acceptable and was retain. Preliminary heat transfer calculations were made to assess the impact of low emissivity coating on the radiative heat transport in the evacuated gap. Other calculations evaluated thermal bridges effects of spacers and water piping with the aim to minimise their impact.

The first work package on concept development is nearly finished. A final validation of the final design concept with the industrial partner will close this step.

Future work concerns activities of work package 2: system integration. This will imply development of a first numerical model of the container VITES with TRNSYS software for thermal behaviour assessment. Annual simulations under different conditions and for different applications (industrial and residential) will follow this. A reference storage will be define with a conventional mineral wool insulation. This allow a comparison between these different insulation technologies.

6 References

[1] Energy Strategy 2050 once the new energy act is in force, OFEN document (2018)

[2] *Energy for the future. Highlights from three years of research at the Swiss Competence Centers for Energy Research (SCCERs).* Topic report (2017)

[3] *Statistique globale suisse de l'énergie*, OFEN (2017)

[4] *Federal Energy Research Masterplan for the period from 2017 to 2020*, CORE (2015)

[5] ECES Annex 30: Thermal Energy Storage for Cost-effective Energy Management and CO_2 Mitigation. www.eces-a30.org

[6] Task 58/ECES Annex 33: Material and Component Development for Thermal Energy Storage. www.task58.iea-shc.org

[7] *IEA SHC Task 42 / ECES Annex 29 - A simple tool for the economic evaluation of thermal energy storages*, SHC (2015)

[8] *The energy technology systems analysis programmes (ETSAP): Technology Brief E17*, IRENA (2013)

[9] *Potential for adsorption technology and possible applications*, THRIVE report (2015)

[10] *Traditional, state-of-the-art and future thermal building insulation materials and solutions – properties, requirements and possibilities*, Jell, B.P., Energy and Buildings 43 (2011)

[11] *Vacuum insulated thermals storage in Sengenthal*, Fuchs, B., Hofbeck, K. and Faulstich, M., 5th Int. renewable Energy Storage, Berlin (2010)

[12] *Heat transport in evacuated perlite powders for super-insulated long-term storages up to 300 °C*, Beikircher, T. and Demharter, M., Journal of Heat Transfer 135 (2013)

[13] *A review of thermal energy storage technologies and control approaches for solar cooling*, Pintaldi, S., Perfumo, C., Sethuvenkatraman, S., White, S. and Rosengarten, S., Renew. Sustain. Energy Rev. 41 (2015)

[14] *Energy conservation through energy storage (ECES) programme*. IEA Brochure (2016)

[15] *Thermal conductivity of vacuum insulation materials for thermal energy stores in solar thermals systems*, Lang, S., Gerschitzka, M., Bauer, D. and Drück, H., Energy Procedia 91 (2016)

[16] *A comprehensive review of thermal energy storage*, Sarbu, I. and Sebarchievici, C., Sustainability 10 (2018)

[17] *Vacuum insulation panels – exciting thermal properties and most challenging applications*, Fricke, J., Schwab, H., Heinemann, U., Int. J. Thermophysics 27 (2006)

[18] *On vacuum insulated thermal storage*, Fuchs, B., Hofbeck, K. and Faulstich, M., Energy Procedia 30 (2012)

[19] *Vacuum super insulated heat storage up to 400 °C*, Beikircher, T., Reuss, M. and Streit, G., Conference paper (2015)

[20] *Thermal energy storage with super insulating materials: a parametrical analysis*, Fantucci, S., Lorenzati, A., Kazas, G., Levchenko, D. and Serale, G., Energie Procedia 78 (2015)

[21] *Vacuum-buffer storage*, HummelsbergerStahl-und Metallbau, www.vacuum-storage.com

[22] *Projet Colas : Campagne de mesures : Installation solaire thermique à haute température de Colas Suisse*, Bunea, M., Duret, A, Péclat, L, Bornet, P., Maranza, M., Wendling, J.-B and Pauletta, S., OFEN Annual report (2014)

[23] *Projet Colas : Campagne de mesures : Installation solaire thermique à haute température de Colas Suisse*, Bunea, M., Hildbrand, C., Duret, and Citherlet, S., OFEN Annual report (2016)

[24] *Anwendungen und potenziale von vakuum spalt isolation*, Tischhauser, H. and Staufert, G., (2013)

[25]*Thermal Energy Storage*, Swiss Competence Center for Energy Research, www.sccer-hae.ch

[26] ANSYS software, www.ansys.com

[27] *Materials for high vacuum technology: an overview*, Sgobba, S., CERN document (2006)

[28] ASM Material Data Sheet

[29] TVP Solar, private communication.

[30] *Introduction to Heat Transfer*, Incropera, F. and de Witt, D., Wiley (1985)

7 Appendix

7.1 Appendix 1: FEA structural analysis report

Project :	VITES			Version: V2
Subject :	Structural analysis			
From :	COMATEC	To :	TVP Solar	Date :
Author(s) :	Oberholzer Stefan BFE			

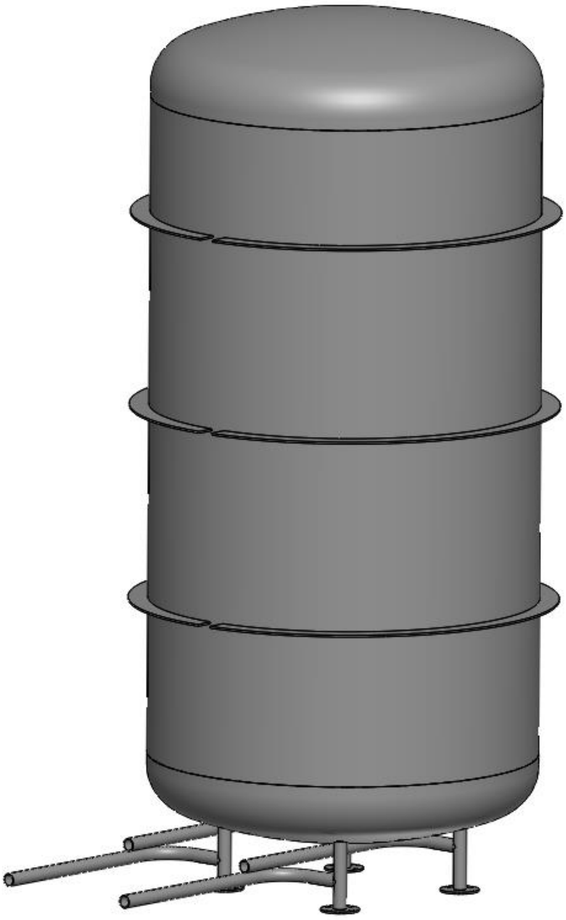

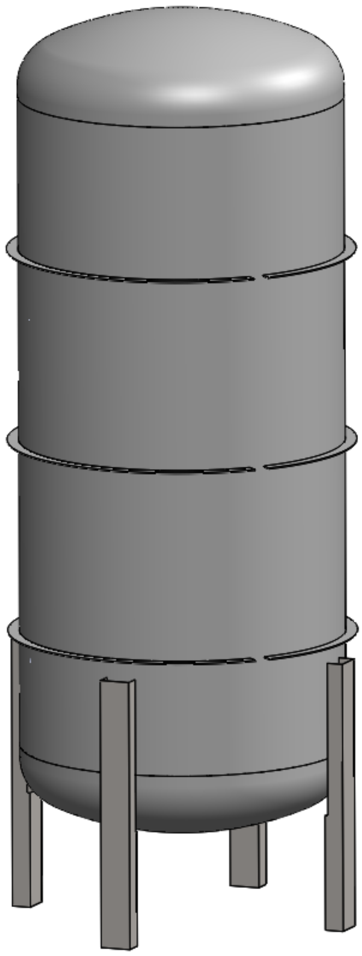

Table of contents

1 Introduction

This report present the geometry and the structural analysis of a tank under vacuum. This tank is made of two tanks, an inner one to contain water and an outer one. The outer tank must allow a vacuum between the two shells to isolate the inner tank and minimize the heat exchange between the water and the exterior.
The characteristics of the tank are:

- Capacity : 1000 [l]
- Minimize the heat exchange
- Four pipes for water circulation
- Attachment points on the top of the tank
- Minimize the gap between the two shells

2 Analytical calculation: formulas

The complete calculation is available in the Excel file "Dimensionnement.xlsx".
The following equations are valid for thin wall tubes. The criteria for thin wall are:

$$\frac{a}{R_m} \leq 0.1 \qquad or \qquad \frac{D_a}{D_i} \leq 1.2$$

Thickness of the wall	a	[mm]
Medium raduis	R_m	[mm]
Outer diameter	D_a	[mm]
Inner diameter	D_i	[mm]

Table 2 : calculation parameters (thin wall)

The minimal wall thickness is determined separately for the cylinder part and the curved bottoms. The following equations are from Decker Maschinenelemente [1].
These values will be use for the 3D model and will be check with the simulation.
The minimal thickness for the wall of the cylinder parts of the two tank is determined with:

$$s_{min} = \frac{D_a \cdot p_i}{2 \cdot \frac{K}{S} \cdot v + p_i} + c$$

For the curved bottoms, the minimal thickness is:

$$s_{min} = \frac{D_a \cdot p_i \cdot \beta}{4 \cdot \frac{K}{S} \cdot v + p_i} + c$$

[2] Any corrosion allowance, which leads to the standard formula commonly used for thin tubes " c"

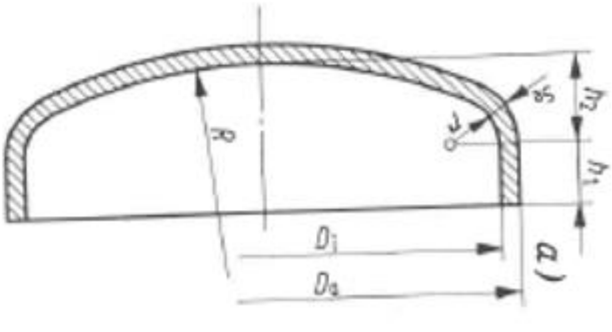

$$r = 0{,}1 D_a, \quad h_1 \geqq 3{,}5 s, \quad h_2 = 0{,}1935 D_a - 0{,}455\, s_e, \quad \frac{s_e - c}{D_a} = 0{,}001 \ldots 0{,}1$$

Figure 3 : geometry of the curved bottom

The parameters of the previous equations are the followings:

Outer diameter	D_a	[mm]
Characteristic of material resistance	K	[MPa]
Security factor	S	[-]
Welding factor	v	[-]
Over thickness	c	[mm]
Inner pressure	p_i	[bar]
Coefficient	β	[-]

Table 3 : Calculation parameters (minimal thickness, Decker Maschinenelemente)

The outer tank must also resist linear buckling. To check the buckling resistance, the critic pressure is determined with the material and geometry parameters. This pressure has to be higher than the working pressure for the tank to resist buckling.
The determination of the critic pressure comes from "Techniques de l'ingénieur : tuyauteries. Résistance des éléments" [3].

.

$$p_{cr} = \frac{2.42 \cdot E}{(1-\mu^2)^{0.75}} \cdot \frac{\left({}^{a}/_{D_e}\right)^{2.5}}{\left({}^{L}/_{D_e}\right) - 0.45 \cdot \left({}^{a}/_{D_e}\right)^{0.5}} \geq x \cdot p_{atm}$$

-Security factor x=3
-Steel μ=0.3

Wall thickness	a	[mm]
Young's modulus	E	[GPa]
Poisson's ratio	μ	[-]
Outer diameter	D_e	[mm]
Distance between reinforcement	L	[mm]
Security factor	x	[-]
Atmospheric pressure	p_{atm}	[bar]
Critic pressure	p_{cr}	[bar]

Table 4 : calculation parameters (critic pressure)

The last verification point is the resistance of the feet (compression and buckling):

$$\sigma_{feet} = \frac{m_{tot} \cdot g}{n \cdot S_{feet}}$$

$$F_k = \frac{\pi^2 \cdot E \cdot I_y}{l_k^2}$$

Constraint in one foot	$\boldsymbol{\sigma_{feet}}$	[MPa]
Total mass (water and tank)	m_{tot}	[kg]
Quantity of feet	n	[-]
Area of one foot	S_{feet}	$[mm^2]$
Young's modulus	E	[GPa]
<u>Second moment of area</u>	I_y	$[mm^4]$
Buckling length	l_k	[mm]
Maximum length of one foot	l	[mm]

Equivalent of Buckling length

$$l_k = 2 \cdot l$$

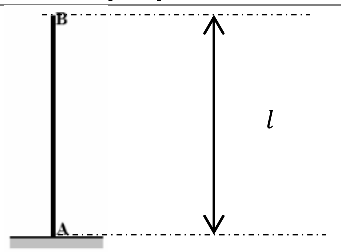

$$l_k = l$$

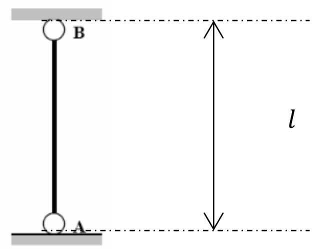

$$l_k = 0.7 \cdot l$$

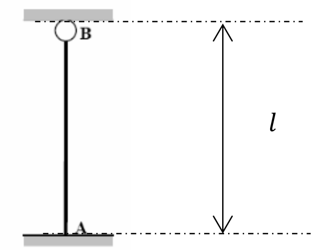

$l_k = 0.5 \cdot l$	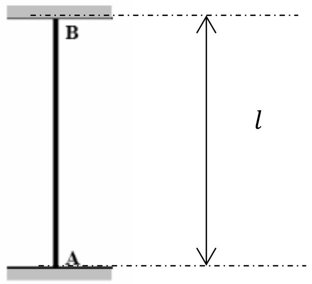

Table 5 : calculation parameters (compression and buckling)

3 Simulation: CODAP criteria [4]

The simulation will be perform on Ansys. The output will be constraint to check the resistance, the deformation and the multiplication factor for the buckling. The different criteria used for the interpretation are visible in Table 6.
The CODAP criteria are used to verify constraint given by the simulation. There are two different type of constraint:

- Primary constraint : constraint that participate at the mechanical equilibrium (forces)
- Secondary constraint : constraint generated by the necessary compatibility of the common deformation of different parts

These two type of constraint can be general or local. General constraint are located on zones that are relatively straight with no sudden geometric variation and local constraint are the one near these variations. The bellowing table shows the criteria for local and general constraint.
$\boldsymbol{R_{p\,1.0}}$ plastic stretching to 1.0%, $\boldsymbol{R_m}$: tensile strength

Type of constraint depending meshing	Linearized constraint	Solid mesh
	Membrane constraint	Shell mesh
Nominal constraint for calculation		$f = min\left\{\left(\frac{R_{p\,1.0}}{1.2}\right);\left(\frac{R_m}{3}\right)\right\}$
		Table in ASMEB31.3-1[5]
Equivalent stress (Tresca)		$\sigma_{eq} = max\{\lvert\sigma_1 - \sigma_2\rvert, \lvert\sigma_2 - \sigma_3\rvert, \lvert\sigma_3 - \sigma_1\rvert\} = 2 \cdot \tau_{max}$
Type of constraint	Primary general constraint (membrane)	$(\sigma_{eq})_{Pm} \leq 1.1 \cdot f$
	Primary local constraint (membrane)	$(\sigma_{eq})_{Pl} > 1.1 \cdot f$
Primary constraint	Primary general constraint (membrane)	$(\sigma_{eq})_{Pm} \leq f$

	Primary local constraint (membrane)	$(\sigma_{eq})_{Pl} \leq 1.5 \cdot f$
	Primary global constraint (membrane and bending)	$(\sigma_{eq})_{P} \leq 1.5 \cdot f$
Local constraint	Local zone without form discontinuity	$l_1 \leq \sqrt{R \cdot e}$
	Local zone around a form discontinuity	$l_1 \leq \dfrac{\sqrt{R_1 \cdot e_1} + \sqrt{R_2 \cdot e_2}}{2}$
	Minimal distance between two local zone	$l_2 \leq 2.5 \cdot \sqrt{R \cdot e}$

Table 6 :CODAP

4 Prototype one

4.1 Overview

This view shows the construction of the tank. The outer tank is reinforced with C parts to resist buckling because of the vacuum between the two tanks. The positioning of the inner tank is made with the four tubes (outer diameter 33.4 [mm], inner diameter 25.4 [mm]) that are welded in the two curved bottoms.

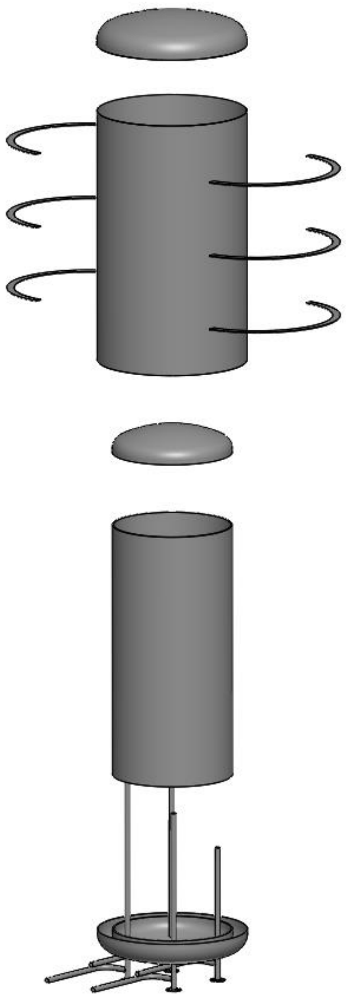

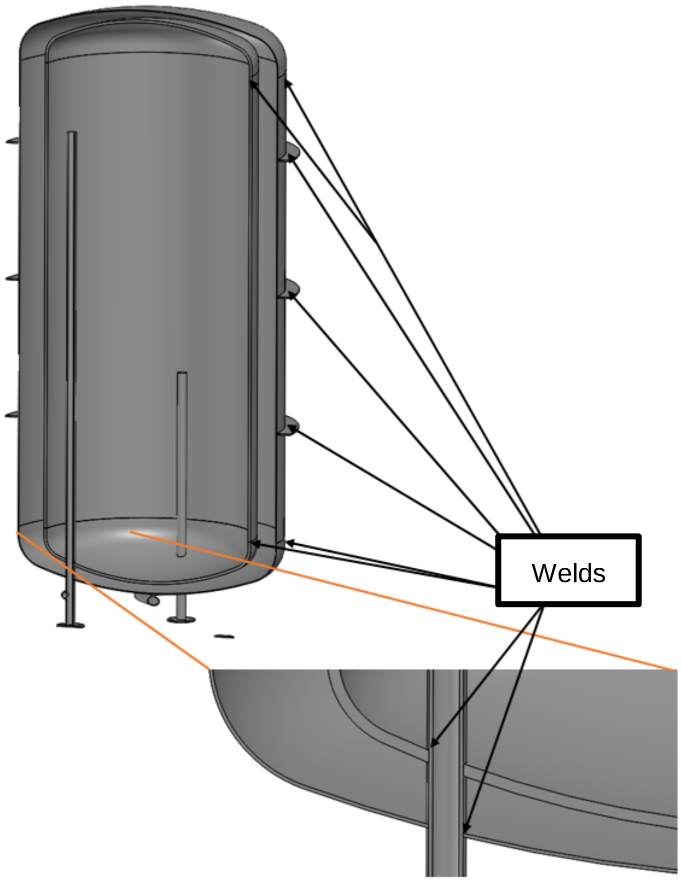

4.2 Analytical calculation

4.2.1 Inner tank

Outer diameter	D_a	800	[mm]
Characteristic of material resistance	K	200	[MPa]
Security factor	S	2	[-]
Welding factor	v	0.8	[-]
Over thickness	c	1.5	[mm]
Inner pressure	p_i	1.6	[MPa]
Minimal thickness	***s_{min}***	***9.3***	***[mm]***

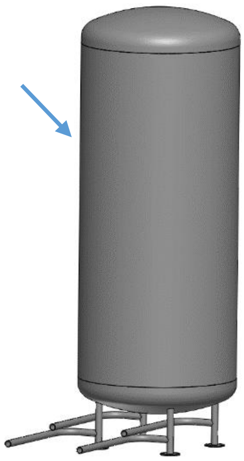

Table 7: inner tank, cylindrical part

Outer diameter	D_a	800	[mm]
Characteristic of material resistance	K	200	[MPa]
Security factor	S	2	[-]
Welding factor	v	0.8	[-]
Over thickness	c	1.6	[mm]
Inner pressure	p_i	1.6	[MPa]
Coefficient	β	4.6	[-]
Minimal thickness	***s_{min}***	***19.9***	***[mm]***

Table 8 : inner tank, curved bottom

The thickness of the two parts will be adapt depending the results of the simulation. The curved bottom and the cylinder part will have different thickness giving the big difference between the two analytical values.

Caractéristique matériau

Type	316L	1.4404
Rp 0.2	220	[MPa]
Rp 1.0		[MPa]
Re		[MPa]
Rm	520	[MPa]

Technical Pocket Guide (Schaffler)

4.2.2 Outer tank

Outer diameter	D_a	1000	[mm]
Characteristic of material resistance	K	200	[MPa]
Security factor	S	2	[-]
Welding factor	v	0.8	[-]
Over thickness	c	1.4	[mm]
Outer pressure	p_e	0.1	[MPa]
Minimal thickness	s_{min}	***2.0***	***[mm]***

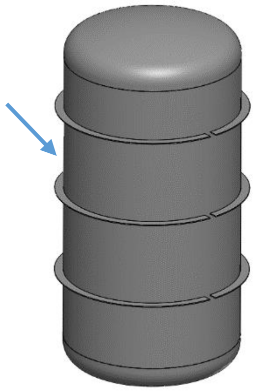

Table 9 : outer tank, cylindrical part

Outer diameter	D_a	1000	[mm]
Characteristic of material resistance	K	200	[MPa]
Security factor	S	2	[-]
Welding factor	v	1	[-]
Over thickness	c	1.4	[mm]
Outer pressure	p_e	0.1	[MPa]
Coefficient	β	4.6	[-]
Minimal thickness	s_{min}	***2.5***	***[mm]***

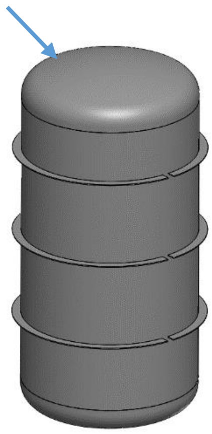

Table 10 : outer tank, curved botom

Outer diameter	D_a	1000	[mm]
Wall thickness	a	3	[mm]
Young's modulus	E	210	[GPa]
Poisson's ratio	v	0.3	[-]
Distance between reinforcement	L	500	[mm]
Critical pressure (with reinforcement)	p_{cr}	***5.66***	***[bar]***

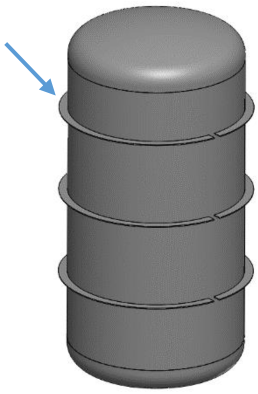

Table 11 : critical pressure (buckling)

For the outer tank, the thickness for the cylinder part and the curved bottom is nearly the same, so a common thickness will be use in the simulation.
The solution with three reinforcement is acceptable because the critical pressure is 5.6 times higher than the atmospheric pressure, pressure that is the same anywhere on earth.

4.2.3 Feet

Tubes			
Outer diameter	R_e	16.7	[mm]
Inner diameter	R_i	12.7	[mm]
Area	S_{feet}	369.5	[mm^2]
Second moment of area	I_y	40656.3	[mm^4]
Quantity of feet	n	4	[-]
Material			
Young's Modulus	E	210	[GPa]
Poisson's ratio	v	0.3	[-]
Load			
Tank mass	m_{res}	664	[kg]
Water mass	m_{eau}	1000	[kg]
Overall weight	F_g	16323.8	[N]
Compression			
Compression constraint	$\boldsymbol{\sigma_{feet}}$	**11.05**	**[MPa]**
Yield strength	F_e	207	[MPa]
Buckling			
Maximal length	l	170	[mm]
Buckling length (case l_k = 0.7 l)	l_k	119	[mm]
Maximal load before buckling	F_k	5866	[N]
Load per foot	$\boldsymbol{F_{g,1}}$	**4081**	**[N]**

Table 12 : feet calculation (compression and buckling)

With four feet, the compression constraint is much lower than the yield strength. The maximal buckling load is 5866 [N], which is 30% higher than the actual load. In conclusion, the use of the water tubes as feet is possible.

4.3 Simulation

4.3.1 Geometry and loads

Mesh	Inner pressure	Outer pressure
Shell, quadrilateral	$p_i = 16\ [bar]$	$p_e = 1\ [bar]$
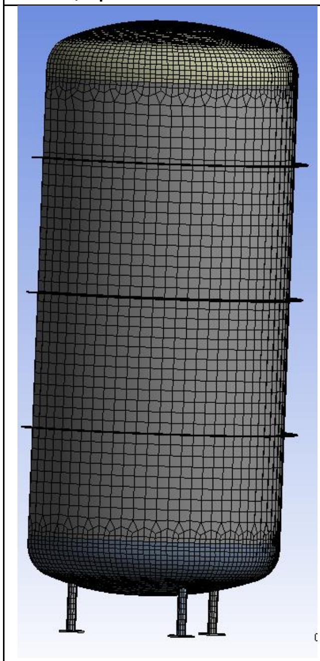	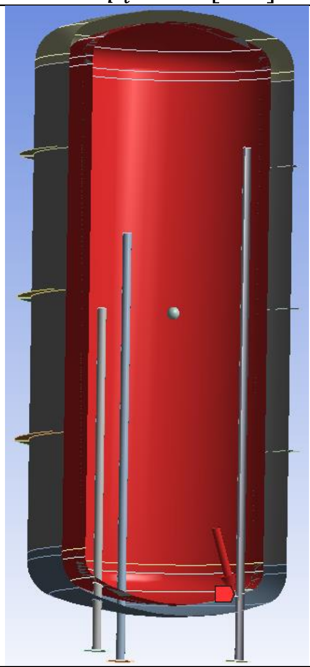	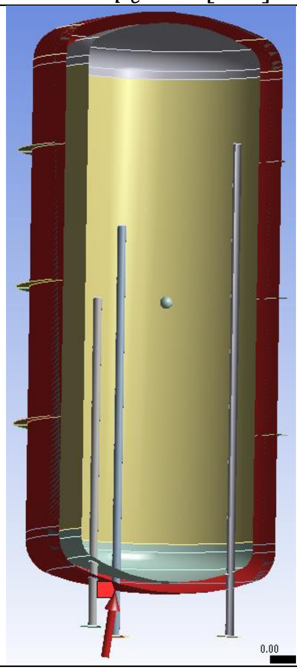

Water	Gravity
$m = 1000\ [kg]$	$g = 9.81\ \left[{}^{m}/{}_{s^2}\right]$

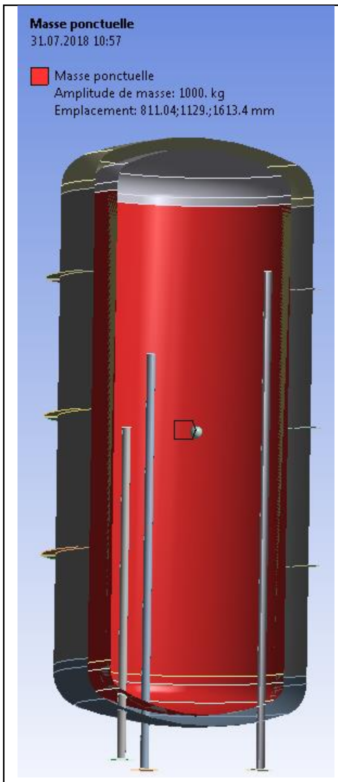	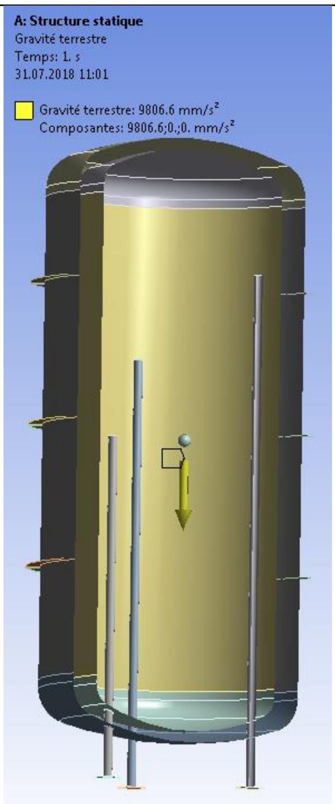

Table 13 : loads, prototype 1

Thickness	
Inner tank, cylindrical part	8 [mm]
Inner tank, top	8 [mm]
Inner tank, bottom	8 [mm]
Outer tank, cylindrical part	3 [mm]
Outer tank, top	3 [mm]
Outer tank, bottom	3 [mm]
C’s reinforcements	3 [mm]
Overall mass	
655 [kg]	

Table 14 : geometry, prototype 1

4.3.2 Shear constraint

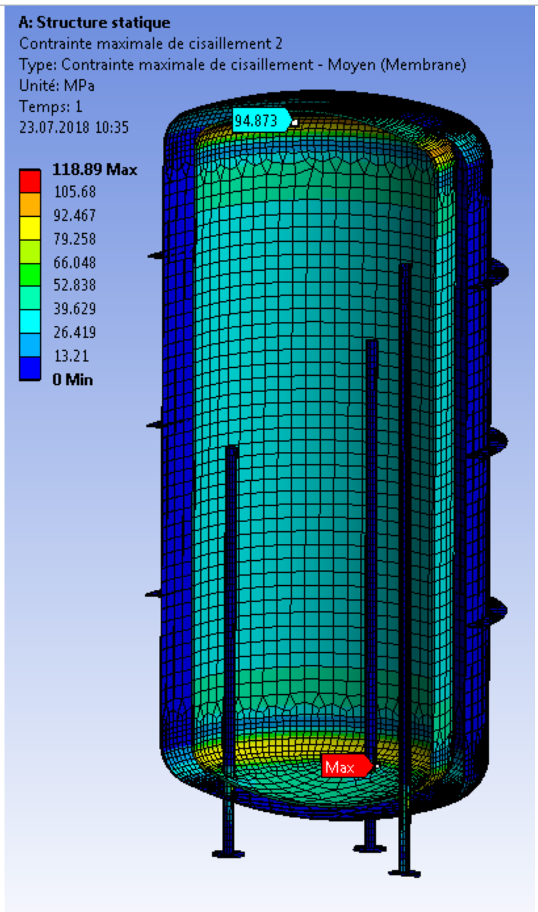

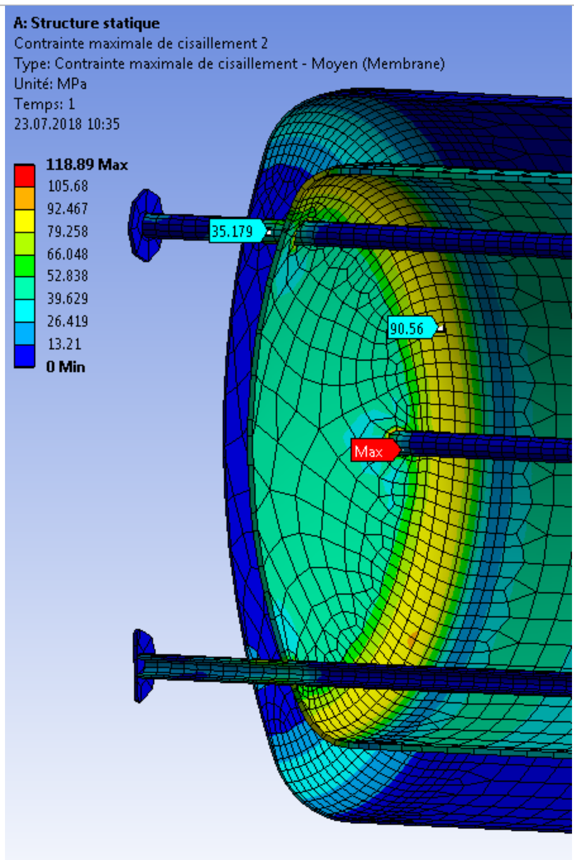

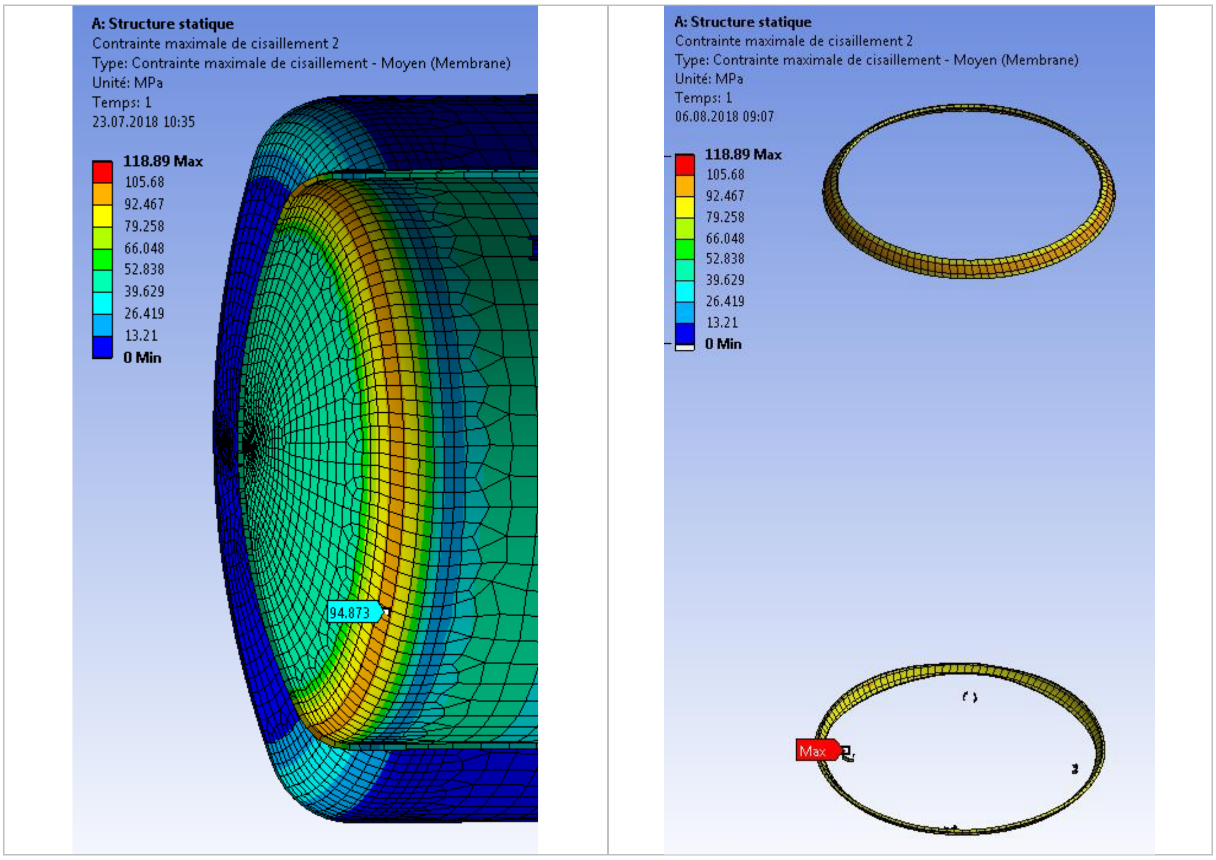

Table 15 : membrane constraint, prototype 1

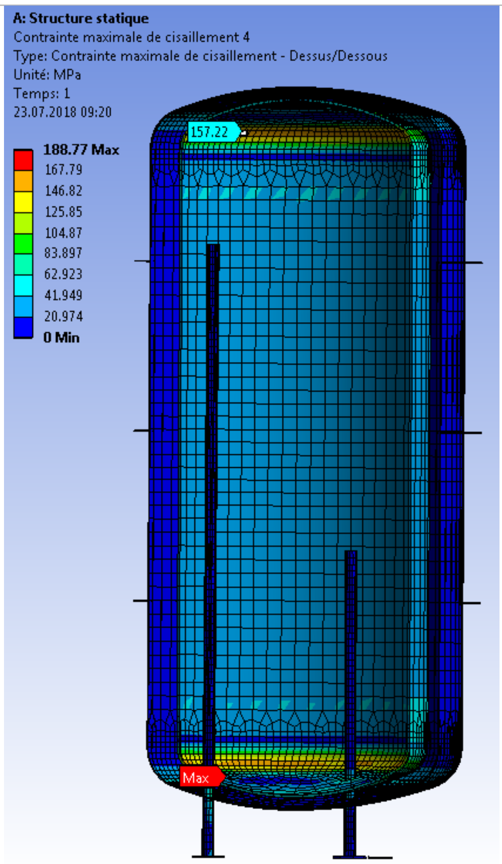
A: Structure statique
Contrainte maximale de cisaillement 4
Type: Contrainte maximale de cisaillement - Dessus/Dessous
Unité: MPa
Temps: 1
23.07.2018 09:20
188.77 Max
167.79
146.82
125.85
104.87
83.897
62.923
41.949
20.974
0 Min
157.22
Max

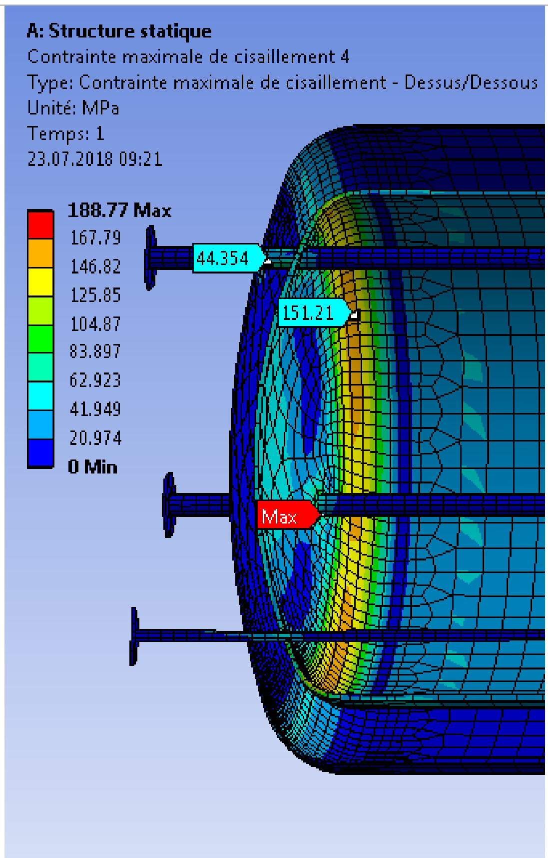
A: Structure statique
Contrainte maximale de cisaillement 4
Type: Contrainte maximale de cisaillement - Dessus/Dessous
Unité: MPa
Temps: 1
23.07.2018 09:21
188.77 Max
167.79
146.82
125.85
104.87
83.897
62.923
41.949
20.974
0 Min
44.354
151.21
Max

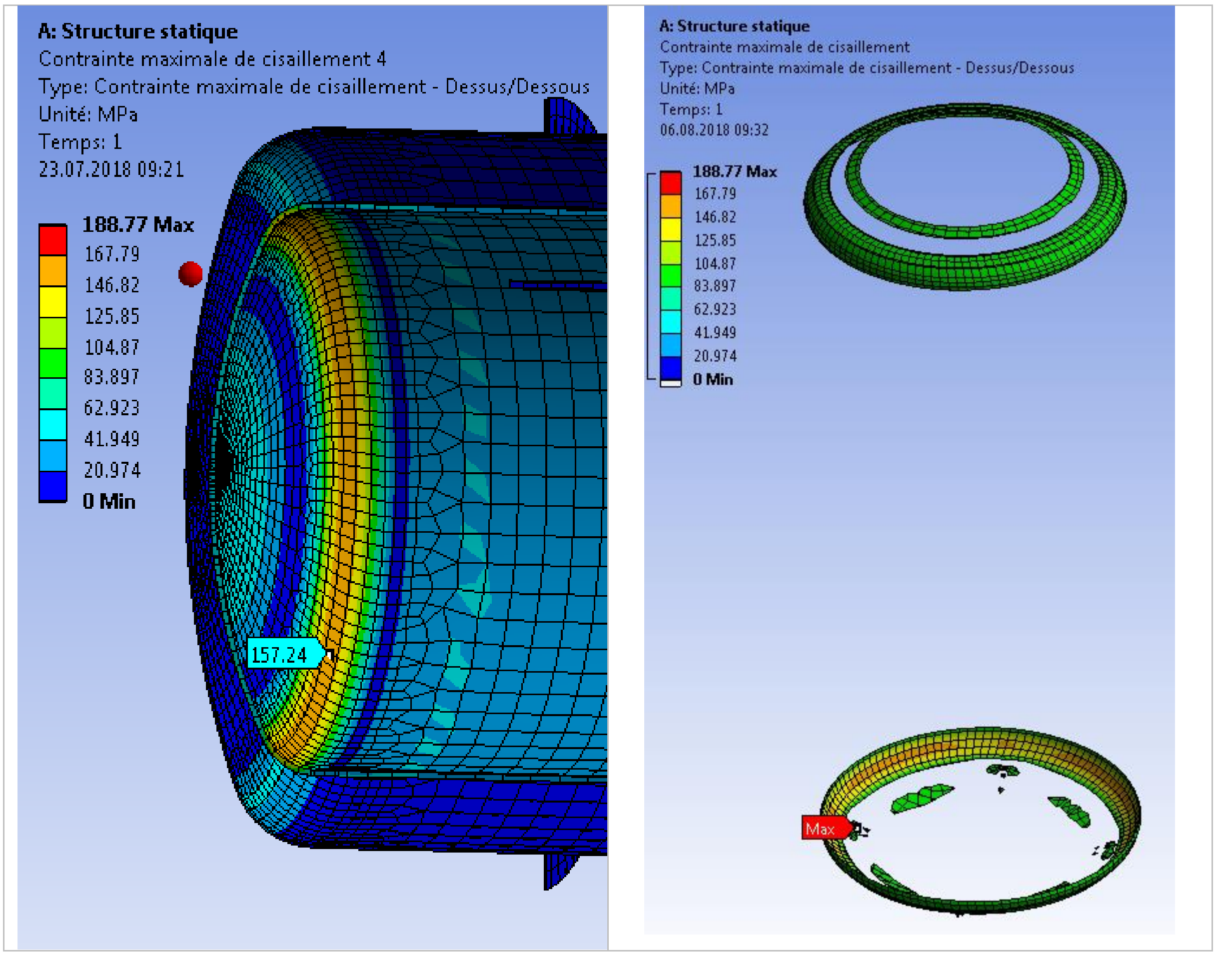

Table 16 : global constraint, prototype 1

<table>
<tr><th colspan="4">Membrane</th></tr>
<tr><td>Primary general constrain</td><td colspan="2">$f = 172.4\ [MPa]$</td><td>$\sigma_{eq} = 2 \cdot \tau_{max} = 2 \cdot 94.873 = 189.746\ [MPa]$</td></tr>
<tr><td>Primary local constrain</td><td colspan="2">$1.5 \cdot f = 258.6\ [MPa]$</td><td>$\sigma_{eq} = 2 \cdot \tau_{max} = 2 \cdot 118.89 = 237.78 [MPa]$</td></tr>
<tr><td colspan="2"></td><td>Theoretical</td><td>Effective</td></tr>
<tr><td rowspan="2">Local zone</td><td>Inner tank</td><td>$l_1 \leq \sqrt{R \cdot e} = 54.8\ [mm]$</td><td>$l_1 \cong 50\ [mm]$</td></tr>
<tr><td>Outer tank</td><td>$l_2 \leq \sqrt{R \cdot e} = 80\ [mm]$</td><td>-</td></tr>
<tr><th colspan="4">Global</th></tr>
<tr><td>Primary global constraint</td><td colspan="2">$1.5 \cdot f = 258.6\ [MPa]$</td><td>$\sigma_{eq} = 2 \cdot \tau_{max} = 2 \cdot 188.77 = 377.54\ [MPa]$</td></tr>
<tr><td colspan="2"></td><td>Theoretical</td><td>Effective</td></tr>
<tr><td>Local zone</td><td>Inner tank</td><td>$l_1 \leq \sqrt{R \cdot e} = 54.8\ [mm]$</td><td>$l_1 \cong 60\ [mm]$</td></tr>
</table>

	Outer tank	$l_2 \leq \sqrt{R \cdot e} = 80\ [mm]$	-

Table 17 : constraints results, prototype 1

Constraints of the major parts is lower than the nominal constraint for calculation. The critical parts are the curved bottom, which constraints are superior to the nominal constraint for calculation. The maximal solicitation is in the welds of the feet.
The local zone (see definition in Table 15) are visible on the last picture of the previous table. The length of these zones is nearly equal to the theoretical length (around 50 [mm] VS 55 [mm]) and the constraints is too high.

4.3.3 Buckling

Mode 1 Load multiplicator : 6.13	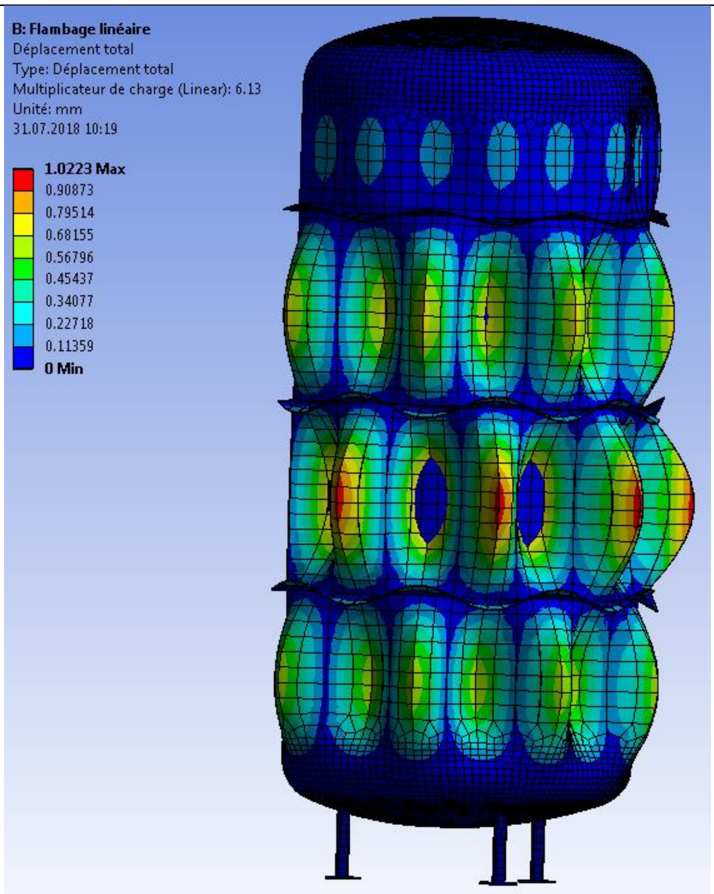

Table 18 : buckling, prototype 1

The minimal buckling load is 6.13 times higher than the nominal load. There is no risk of buckling of the structure with the actual load parameters.

4.3.4 Displacement

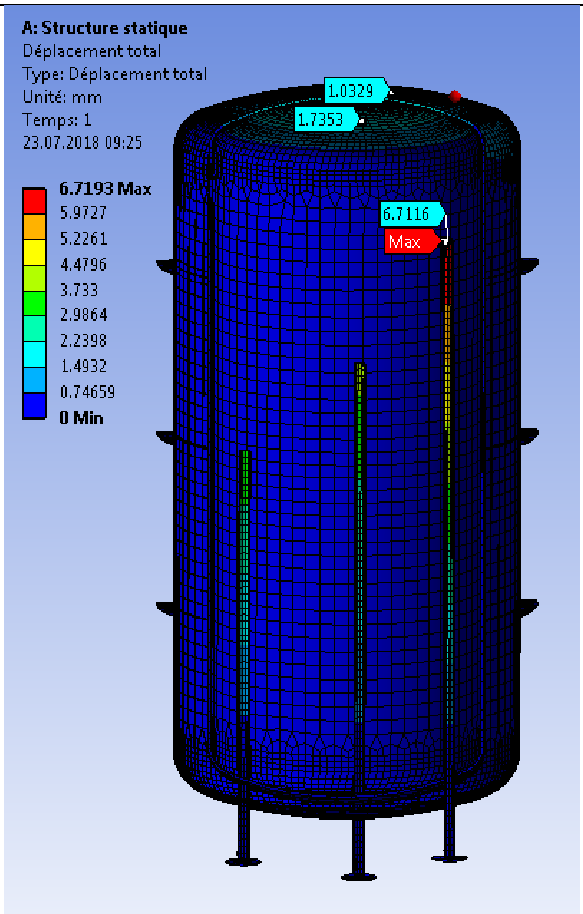

Table 19 : displacement, prototype 1

The major displacement is at the top of the higher tube. This large displacement isn't critical because the tube bend on the inside of the tank and the constraints aren't high in the tube (the displacement is due to de deformation of the inner curved bottom).
The displacement of the top of the tank is acceptable as well because the inner tank does not interfere with the outer tank.

5 Conclusion

The prototype 1 is good regarding buckling but the constraint in the small radius of the inner tank and the welds of the tubes are too high (plastic deformation at these location). This prototype cannot be use as an industrial solution because of its lack of resistance.

6 Prototype two

6.1 Overview

As the first prototype, the outer tank is reinforced with C parts to resist. The positioning of the inner tank in the outer tank is made with radial tubes welded at the inner side of the outer tank and the outer side of the inner tank. These little tubes are only located on the cylindrical parts to simplify the building. The feet are weld outside cylindrical part of the outer tank.
This second prototype uses different thickness for the cylinder and curved parts of the inner tank in order to minimize constraints in the smaller radius of the curved part.

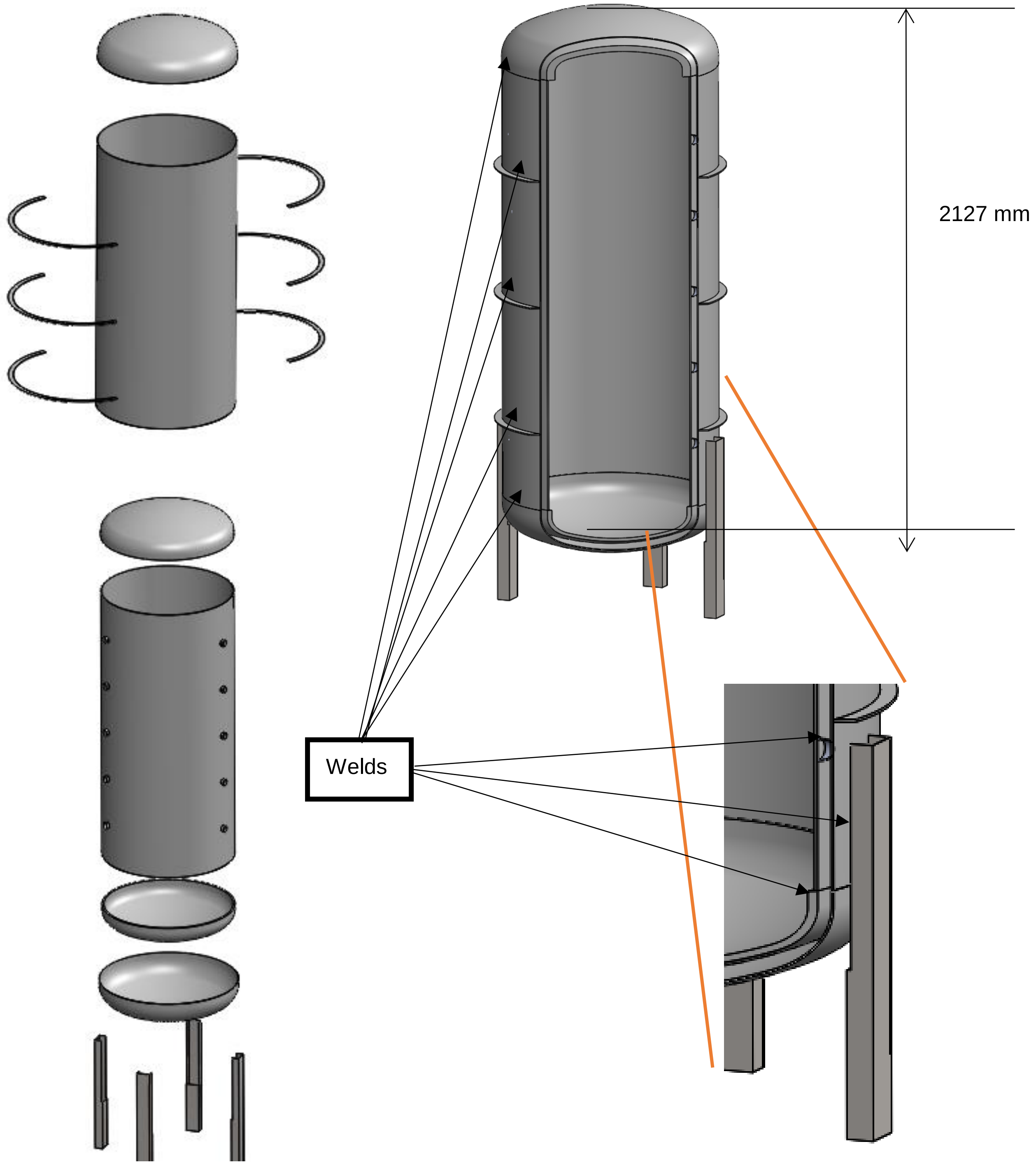

Figure 5 : overview prototype 2 of 15 spaces

6.2 Analytical calculation

6.2.1 Inner tank

Outer diameter	D_a	800	[mm]
Characteristic of material resistance	K	200	[MPa]
Security factor	S	2	[-]
Welding factor	v	0.8	[-]
Over thickness [2]	c	1.5	[mm]
Inner pressure	p_i	1.6	[MPa]
Minimal thickness	***s_{min}***	***9.3***	***[mm]***

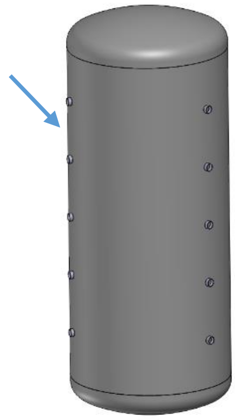

Table 20: inner tank, cylindrical part

Outer diameter	D_a	800	[mm]
Characteristic of material resistance	K	200	[MPa]
Security factor	S	2	[-]
Welding factor	v	0.8	[-]
Over thickness	c	1.6	[mm]
Inner pressure	p_i	1.6	[MPa]
Coefficient	β	4.6	[-]
Minimal thickness	***s_{min}***	***19.9***	***[mm]***

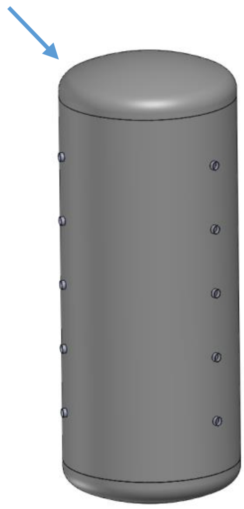

Table 21 : inner tank, curved bottom

The thickness of the two parts will be adapt depending the results of the simulation. The curved bottom and the cylinder part will have different thickness giving the big difference between the two analytical values.

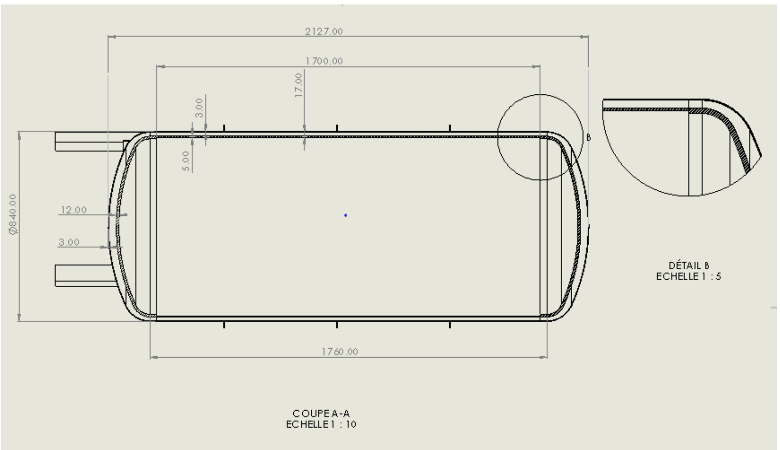
2127.00
1700.00
17.00
3.00
5.00
Ø840.00
12.00
3.00
1760.00
B
DÉTAIL B
ECHELLE 1 : 5
COUPE A-A
ECHELLE 1 : 10

6.2.2 Outer tank

Outer diameter	D_a	1000	[mm]
Characteristic of material resistance	K	200	[MPa]
Security factor	S	2	[-]
Welding factor	v	0.8	[-]
Over thickness	c	1.4	[mm]
Outer pressure	p_e	0.1	[MPa]
Minimal thickness	***s_{min}***	***2.0***	***[mm]***

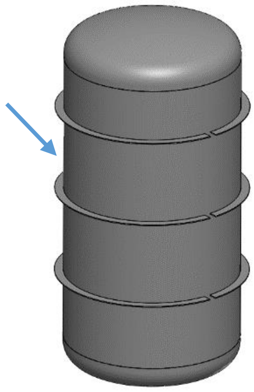

Table 22 : outer tank, cylindrical part

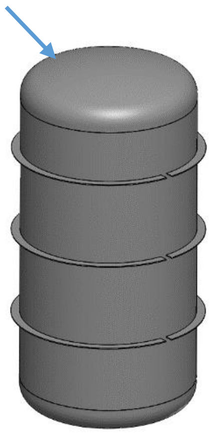

Outer diameter	D_a	1000	[mm]
Characteristic of material resistance	K	200	[MPa]
Security factor	S	2	[-]
Welding factor	v	1	[-]
Over thickness	c	1.4	[mm]
Outer pressure	p_e	0.1	[MPa]
Coefficient	β	4.6	[-]
Minimal thickness	***s_{min}***	***2.5***	***[mm]***

Table 23 : outer tank, curved botom

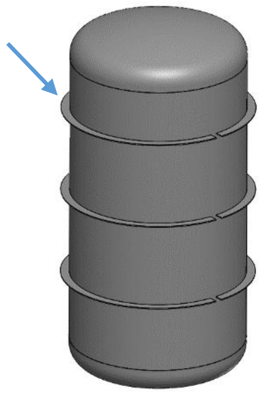

Outer diameter	D_a	1000	[mm]
Wall thickness	a	3	[mm]
Young’s modulus	E	210	[GPa]
Poisson’s ratio	ν	0.3	[-]
Distance between reinforcement	L	500	[mm]
Critical pressure (with reinforcement)	***p_{cr}***	***5.66***	***[bar]***

Table 24 : critical pressure (buckling)

For the outer tank, the thickness for the cylinder part and the curved bottom is nearly the same, so a common thickness will be use in the simulation.
The solution with three reinforcement is acceptable because the critical pressure is 5.6 times higher than the atmospheric pressure, pressure that is the same anywhere on earth.

6.2.3 Feet

Geometry			
External side	x_{e1}	80	[mm]
	x_{e2}	50	[mm]
Internal side	x_{i1}	76	[mm]
	x_{i2}	46	[mm]
Area	S_{feet}	504.0	[mm²]
Second moment of area	I_y	216872.0	[mm⁴]
Quantity of feet	n	4	[-]
Material			
Young's Modulus	E	210	[GPa]
Poisson's ratio	v	0.3	[-]
Load			
Tank mass	m_{res}	664	[kg]
Water mass	m_{eau}	1000	[kg]
Overall weight	F_g	16323.8	[N]
Compression			
Compression constraint	σ_{feet}	**8.10**	**[MPa]**
Yield strength	F_e	207	[MPa]
Buckling			
Maximal length	l	450	[mm]
Buckling length (case l_k = 0.7 l)	l_k	315	[mm]
Maximal load before buckling	F_k	4465	[N]
Load per foot	$F_{g,1}$	**4081**	**[N]**

Table 25 : feet calculation (compression and buckling)

With four feet, the compression constraint is much lower than the yield strength. The maximal buckling load is 4465 [N], which is 10% higher than the actual load.

6.3 Simulation

6.3.1 Geometry

Mesh	Inner pressure	Outer pressure
Shell, quadrilateral	$p_i = 16\ [bar]$	$p_e = 1\ [bar]$
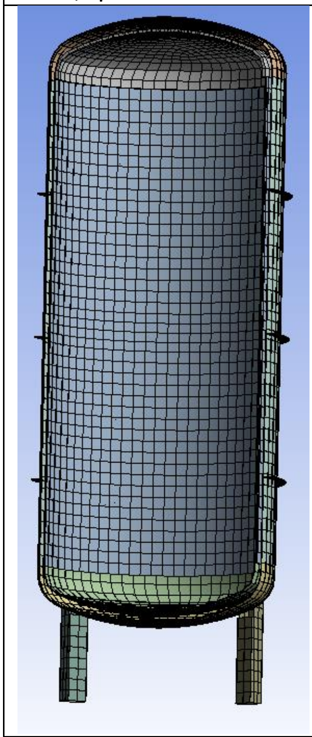	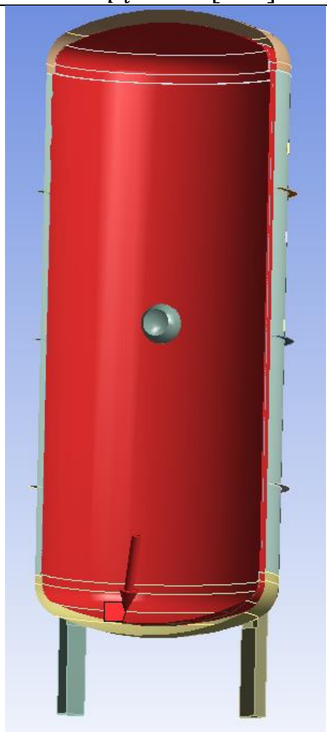	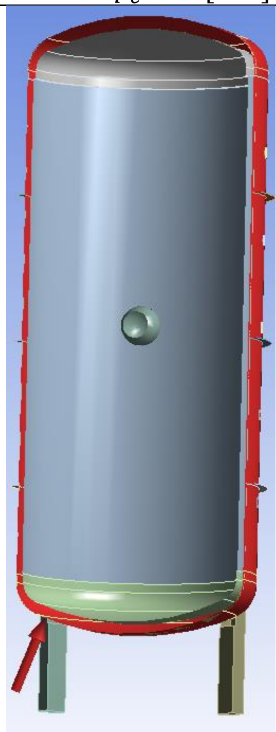

Water	Gravity
$m = 1000\ [kg]$	$g = 9.81\ \left[{}^{m}/_{s^2}\right]$

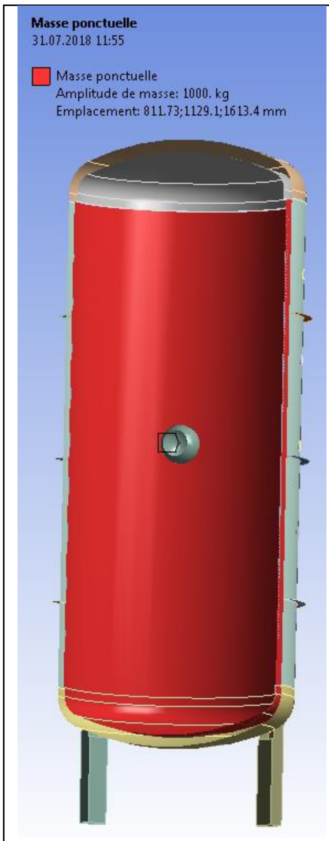

Table 26 : loads, prototype 2

Thickness	
Inner tank, cylindrical part	5 [mm]
Inner tank, top	12 [mm]
Inner tank, bottom	12 [mm]
Outer tank, cylindrical part	3 [mm]
Outer tank, top	3 [mm]
Outer tank, bottom	3 [mm]
C's reinforcements	3 [mm]
Feet	2 [mm]
Overall mass	
462 [kg]	

Table 27 : geometry, prototype 2

6.3.2 Shear constraint

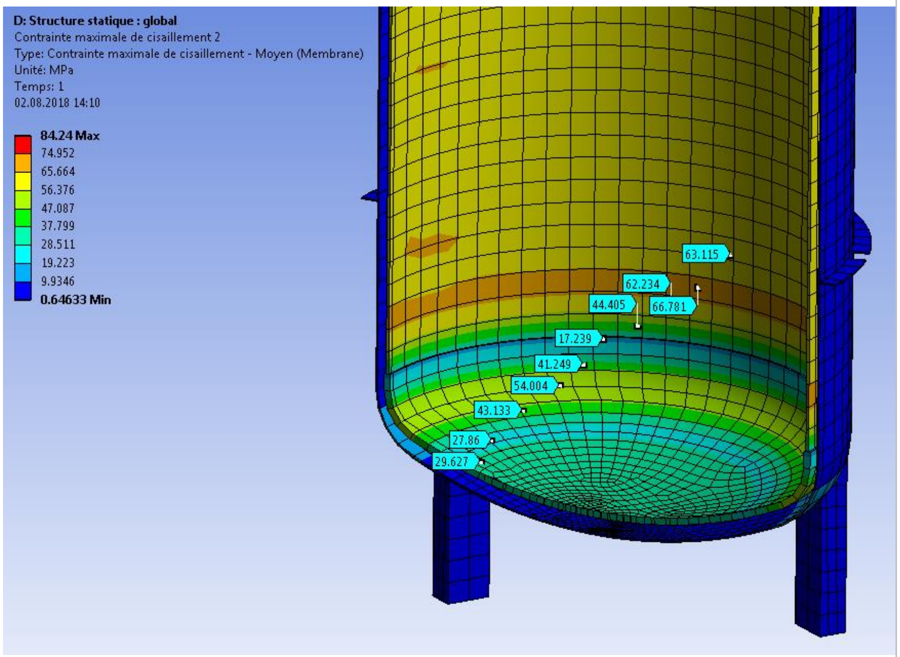

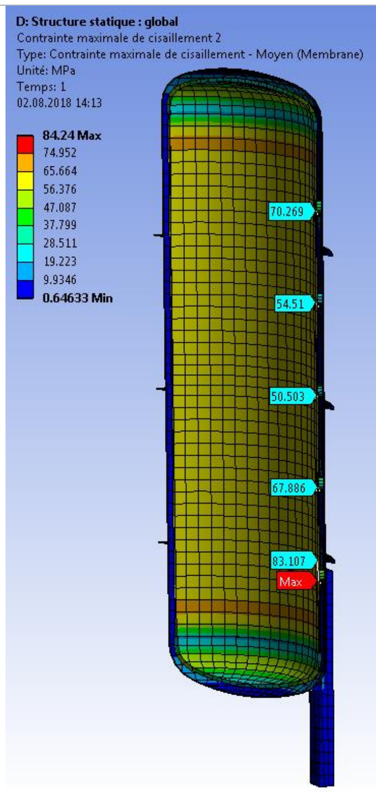

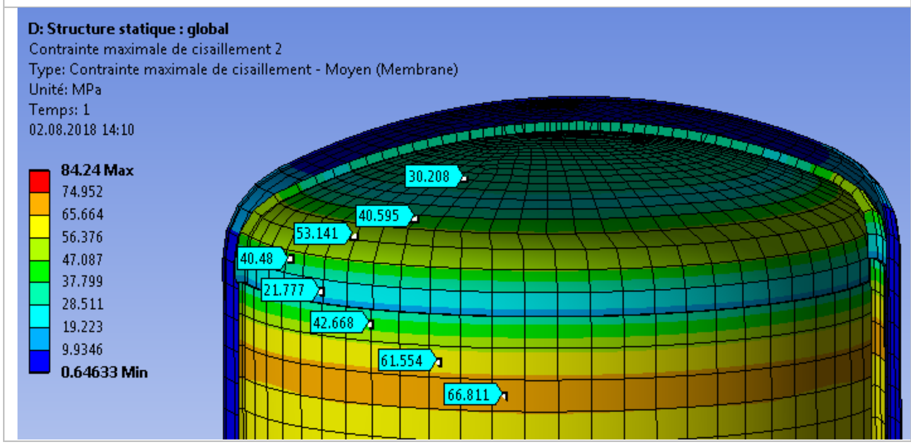

-

Table 28 : membrane constraint, prototype 2

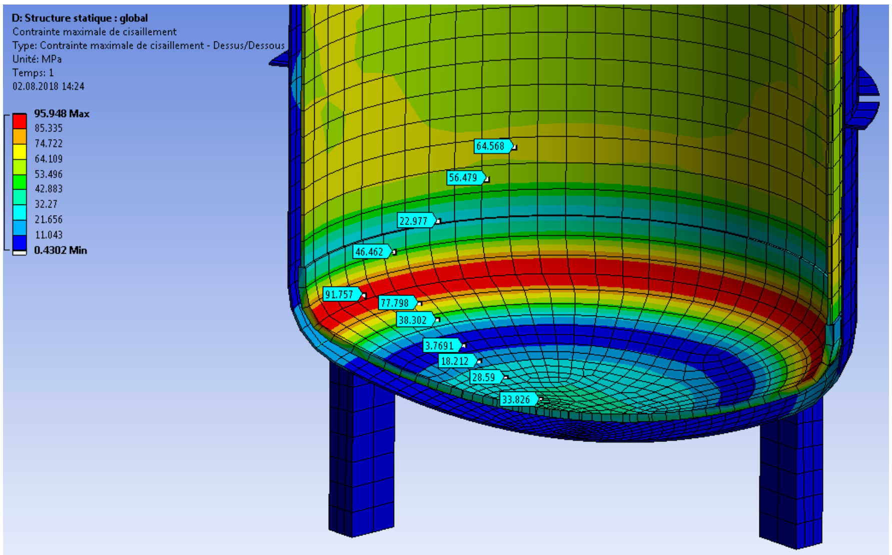

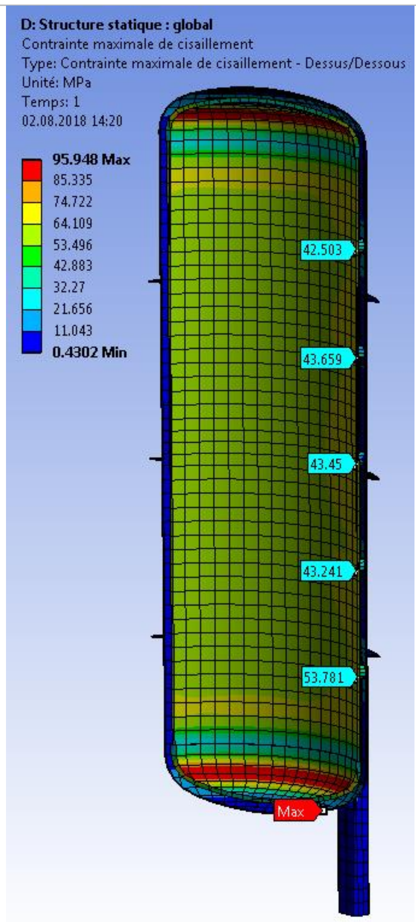

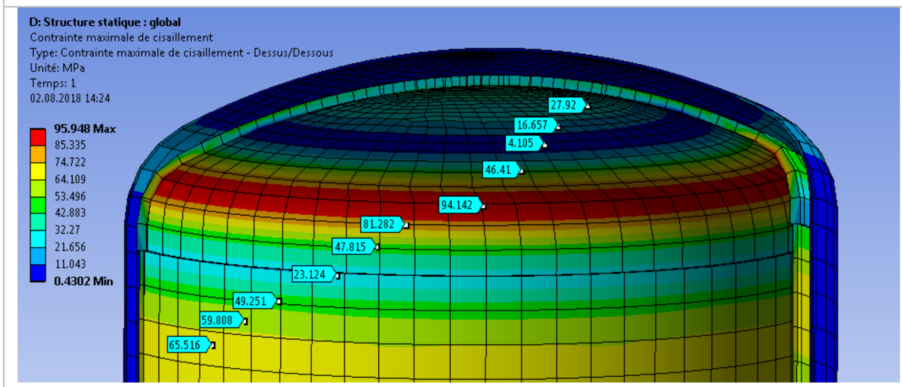

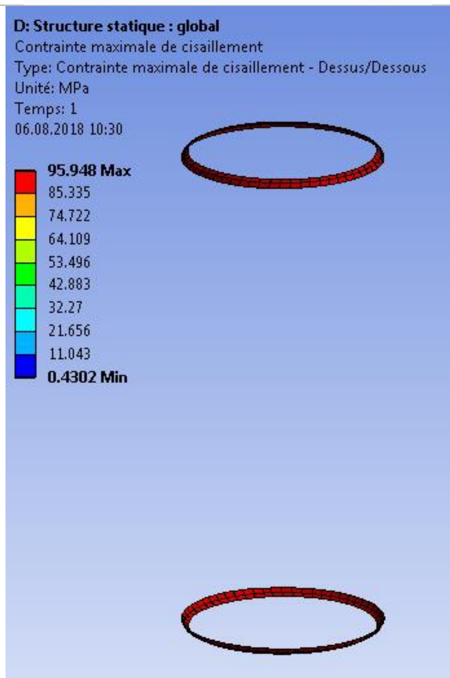

Table 29 : global constraint, prototype 2

Membrane				
Primary general constraint		$f = 172.4\ [MPa]$	$\sigma_{eq} = 2 \cdot \tau_{max} = 2 \cdot 66.8 = 133.6\ [MPa]$	
Primary local constraint		$1.5 \cdot f = 258.6\ [MPa]$	$\sigma_{eq} = 2 \cdot \tau_{max} = 2 \cdot 84.24 = 168.48\ [MPa]$	
		Theoretical	Effective	
Local zone	Inner tank	$l_1 \leq \sqrt{R \cdot e} = 54.8\ [mm]$	-	
	Outer tank	$l_2 \leq \sqrt{R \cdot e} = 80\ [mm]$	-	
Global				
Primary global constraint		$1.5 \cdot f = 258.6\ [MPa]$	$\sigma_{eq} = 2 \cdot \tau_{max} = 2 \cdot 95.948 = 191.896\ [MPa]$	
		Theoretical	Effective	
Local zone	Inner tank	$l_1 \leq \sqrt{R \cdot e} = 54.8\ [mm]$	$l_1 \cong 40\ [mm]$	
	Outer tank	$l_2 \leq \sqrt{R \cdot e} = 80\ [mm]$	-	

Table 30 : constraints results, prototype 2

The membrane constraint are lower than the primary general constraint so there is no local zone regarding this sort of constraint and. The global constraint is good too, being lower than the primary global constraint. There is a local zone here but its length is smaller than the maximal length for local zone.

The cylindrical connectors (connecting the two tanks) have a maximal shear constraint of 54 [MPa]. This does not allow the use of borosilicate glass for these parts because of its lack of resistance, but stainless steel is possible. The heat transfer will be higher but the resistance will be sufficient.

An alternative should be to use cylindrical connectors at the top and bottom and use borosilicate glass instead of stainless steel.

6.3.3 Buckling

Mode 1 Load multiplicator : 9.6	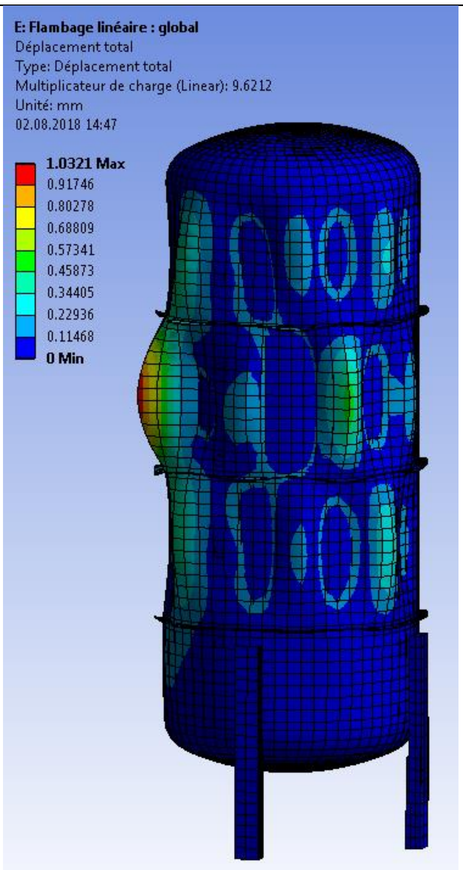

Table 31 : buckling, prototype 2

The minimal buckling load is 9.6 times higher than the nominal load and 1.5 times more than prototype 1. There is no risk of buckling of the structure with the actual load parameters.

6.3.4 Displacement

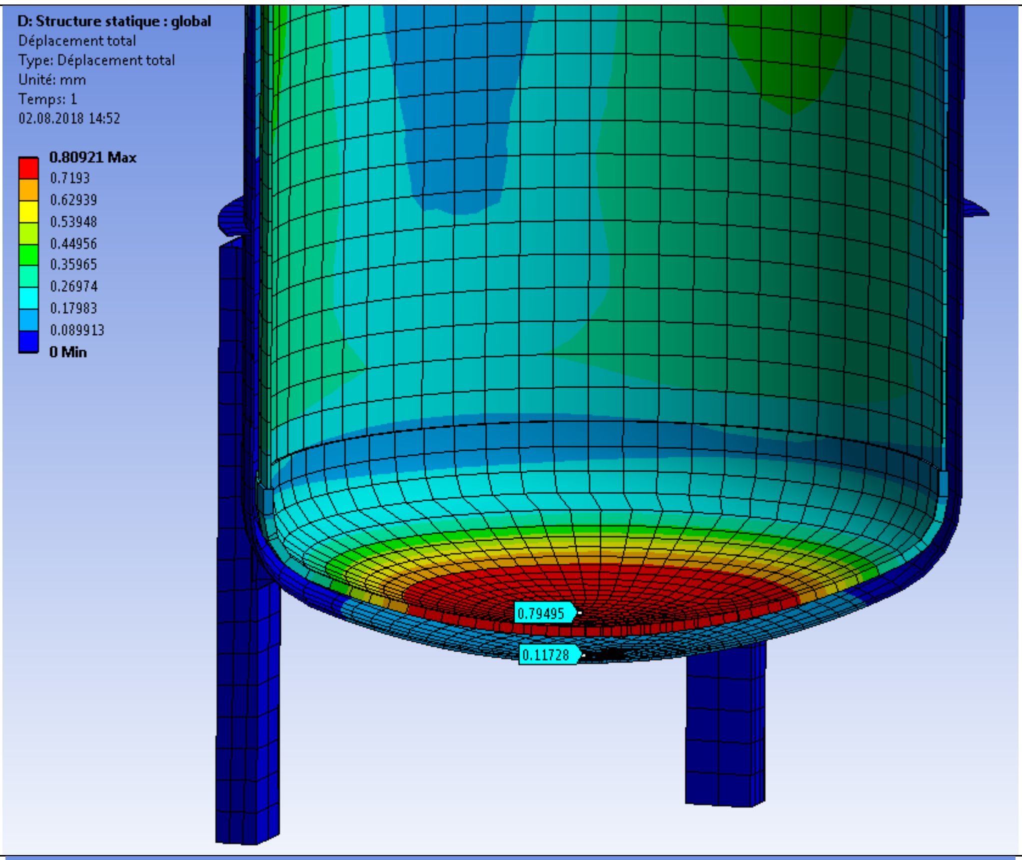

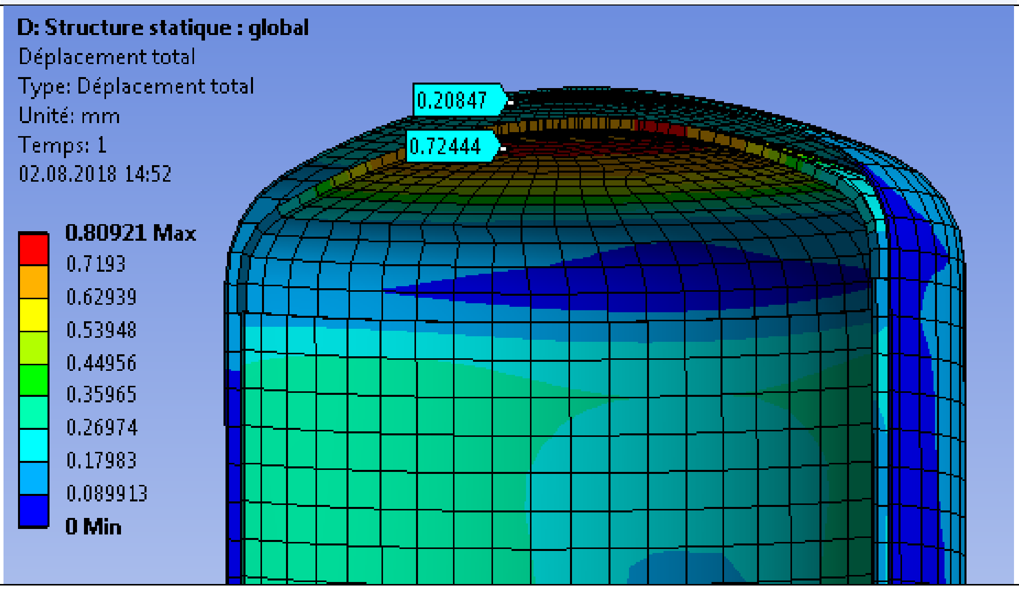

Table 32 : displacement, prototype 2

The biggest displacement is at the top and bottom of the inner tank. These values for displacement are acceptable here because there is no contact between the inner tank and the outer tank. There is also no plastic deformation here, not like in prototype 1.

7 Conclusion

This prototype is better than the first one, having lower constraint and higher buckling factor. The mass has been reduce for about 200 kg compared to prototype 1.

8 Comparison

<table>
<tr><td colspan="2">Prototype 1</td><td colspan="2">Prototype 2</td></tr>
<tr><td colspan="4">Mass</td></tr>
<tr><td colspan="2">655 [kg]</td><td colspan="2">462 [kg]</td></tr>
<tr><td colspan="4">Stress (global)</td></tr>
<tr><td>Inner tank</td><td>Pipe welds</td><td>Inner tank</td><td>Cylindrical reinforcements</td></tr>
<tr><td>314.4[MPa]</td><td>377.5 [MPa]</td><td>191.8 [MPa]</td><td>108 [MPa]</td></tr>
<tr><td colspan="4">Stress (membrane)</td></tr>
<tr><td>Inner tank</td><td>Pipe welds</td><td>Inner tank</td><td>Cylindrical reinforcements</td></tr>
<tr><td>189.7 [MPa]</td><td>237.7 [MPa]</td><td>133.6 [MPa]</td><td>168 [MPa]</td></tr>
<tr><td colspan="4">Load multiplication (buckling)</td></tr>
<tr><td colspan="2">6.2</td><td colspan="2">9.6</td></tr>
</table>

9 Table

10 Figure

11 Annexes

[1] Von Karl-Heinz Decker. *Maschinenelemente Gestaltung und Berechnung, 1990.*

Tab. A 4.26 Sicherheitsbeiwerte S und Wanddickenzuschläge c für Druckbehälter und Dampfkessel (nach AD-Merkblatt A0)

Sicherheitsbeiwert S	bei Walz- und Schmiedestählen	bei Stahlguß
	unter innerem Überdruck 1,5	2
	unter äußerem Überdruck 1,8	2,4
Wanddickenzuschlag $c = c_1 + c_2$		
c_1 Zuschlag zur Berücksichtigung von Wanddickenunterschreitungen: Minustoleranz nach der Maßnorm DIN 1543 bei Blechen von 3 bis unter 8 mm **0,4 mm** 8 15 mm **0,5 mm** 15 25 mm **0,6 mm** bei Rohren ≈ 15% der Wanddicke	von 25 bis unter 40 mm **0,8 mm** 40 80 mm **1,0 mm** 80 150 mm **1,0 mm**	
c_2 Abnutzungszuschlag: bei ferritischen Stählen = 1 mm. Er entfällt bei $s_e \geqq 30$ mm, bei Rohren und bei ausreichendem Schutz durch Verbleiung, Gummierung, Kunststoffüberzügen, bei austenitischen Stählen und bei Nichteisenmetallen. Galvanische Überzüge gelten nicht als Schutz. Bei stark korrodierendem Beschickungsmittel ist ein höherer Zuschlag als 1 mm zu vereinbaren.		

Tab. 4.23 Berechnungsbeiwerte β für gewölbte Böden, gültig für den gesamten Kalotten- und Krempenteil, bei $d_i/D_a = 0$ nur für den Krempenteil (zusammengestellt nach AD-Merkblatt B3)

$\frac{s_e - c}{D_a}$	**Klöpperboden** d_i/D_a							
	0	0,15	0,2	0,25	0,3	0,4	0,5	0,6
0,001	6	7	8					
0,002	4,6	5,4	6,1	7	8,2			
0,003	3,9	4,6	5,3	6,1	7	9		
0,004	3,6	4,3	4,8	5,6	6,3	7,9		
0,005	3,3	4	4,5	5,2	5,9	7,3	8,7	
0,01	2,7	3,3	3,7	4,3	4,7	5,7	6,6	7,5
0,02	2,6	2,9	3,3	3,5	3,8	4,5	5,2	5,9
0,03	2,5	2,9	2,9	3,2	3,4	4	4,6	5,3
0,04	2,5	2,8	2,8	3	3,3	3,7	4,3	4,7
0,05	2,4	2,8	2,8	2,9	3,2	3,5	3,9	4,4
0,1	2,4	2,8	2,8	2,9	2,9	3	3,4	3,7

$\frac{s_e - c}{D_a}$	**Korbbogenboden** d_i/D_a								
	0	0,1	0,15	0,2	0,25	0,3	0,4	0,5	0,6
0,001	3,2	4,2	5,6	7,1	9				
0,002	2,7	3,4	4,5	5,5	6,4	7,5			
0,003	2,4	3	3,9	4,7	5,6	6,4	8		
0,004	2,3	2,8	3,6	4,3	5	5,7	7,2	8,8	
0,005	2,2	2,6	3,4	4	4,6	5,3	6,5	8	
0,01	1,9	2,3	2,8	3,2	3,8	4,2	5	6	6,9
0,02	1,8	2,3	2,5	2,7	3,1	3,4	4	4,7	5,3
0,03	1,8	2,2	2,5	2,6	2,7	3	3,6	4	4,7
0,04	1,7	2,2	2,4	2,5	2,6	2,8	3,3	3,7	4,3
0,05	1,7	2,2	2,4	2,4	2,4	2,6	3,2	3,5	4
0,1	1,7	2,2	2,4	2,4	2,4	2,6	2,7	2,9	3,2

Tab. A 4.25 Festigkeitskennwert K in N/mm^2 von Rohrwerkstoffen und Stahlguß (Auszug aus den DIN-Normen)

Stahlsorte		Dicke mm über	Dicke mm bis	Streckgrenze bei °C 50	100	150	0,2%-Dehngrenze bei °C 200	250	300	350	400	450	500
Warmfeste Stähle DIN 17175	St 35.8		16	235	218	202	185	165	140	120	110	105	
		16	40	225	210	195	180	160	135	120	110	105	
	St 45.8		16	255	238	222	205	185	160	140	130	125	
		16	40	245	228	212	195	175	155	135	130	125	
	17 Mn 4		40	270	258	247	235	215	175	155	145	135	
	19 Mn 5		40	310	292	273	255	235	206	180	160	150	
	15 Mo 3		10	285	270	255	240	220	195	185	175	170	165
		10	40	270	255	240	225	205	180	170	160	155	150
	13 CrMo 4 4		10	305	288	272	255	245	230	215	205	195	190
		10	40	290	273	257	240	230	215	200	190	180	175
	10 CrMo 9 10		40	280	268	257	245	240	230	215	205	195	185
	14 MoV 6 3		40	320	303	287	270	255	230	215	200	185	170
Unlegierte Stähle DIN 1626, 1628, 1629, 1630	St 37.0 und St 37.4		16	235	218	202	185	165	140				
		16	40	225	208	192	175	155	135				
	St 44.0 und St 44.4		16	275	248	232	215	195	165				
		16	40	265	245	225	205	185	160				
	St 52.0 und St 52.4		16	355	318	282	245	225	195				
		16	40	345	308	272	235	215	190				

Stahlgußsorte		0,2%-Dehngrenze bei °C 20	50	100	150	200	250	300	350	400	450	500	550
Warmfester Stahlguß DIN 17245	GS-C25	245	245	222	198	175	160	145	135	130	125		
	GS-22Mo4	245	245	227	208	190	177	165	155	150	145	135	
	GS-17CrMo55	315	315	295	275	255	242	230	215	205	190	180	160
	GS-18CrMo910	400	400	385	370	355	350	345	330	315	305	280	240
	GS-17CrMoV511	440	440	422	403	385	375	365	350	335	320	300	260
	G-X8CrNi12	355	355	328	302	275	270	265	260	255			
	G-X22CrMoV121	590	590	560	530	500	485	470	460	445	420	365	300

Tab. A 4.24 Festigkeitskennwert K in N/mm^2 von Blechwerkstoffen (Auszug aus den DIN-Normen)

	Stahlsorte	Dicke mm über	Dicke mm bis	Streckgrenze bei °C 50	100	150	0,2%-Dehngrenze bei °C 200	250	300	350	400	450	500
Warmfeste Stähle DIN 17155	**UH I**	 16 40	16 40 60	195 185 175	175 168 162	155 152 148	135	115	95	80	70		
	H I	 16 40	16 40 60	235 225 215	218 210 202	202 195 188	185 180 175	165 165 165	140 135 135	120 120 120	110 110 110	105 105 105	
	H II	 16 40	16 40 60	265 255 245	245 238 232	225 222 218	205	185	155	140	130	125	
	17 Mn 4	 16 40	16 40 60	290 285 280	275 272 268	260 258 257	245	225	205	175	155	135	
	19 Mn 6	 16 40	16 40 60	355 345 335	325 318 312	295 292 288	265	245	225	205	175	155	
	15 Mo 3	 10 40	10 40 60	285 270 260	270 255 243	255 240 223	240 225 210	220 205 195	195 180 170	185 170 160	175 160 150	170 155 145	165 150 140
	13 CrMo 4 4	 10 40	10 40 60	300 295 295	285 280 273	270 265 252	255 240 230	245 230 220	230 215 205	215 200 190	205 190 180	195 180 170	190 175 165
	10 CrMo 9 10	 16 40	16 40 60	310 300 290	288 282 272	267 263 253	245 235	240 230	230 220	215 205	205 195	195 185	185 175
Feinkornbaustähle DIN 17102	**WSt 255**	 35	35 70	255 235	226 216	206 201	186	167	137	118	108		
	WSt 285	 35	35 70	285 265	255 245	235 226	206	186	157	137	118		
	WSt 315	 35	35 70	315 295	275 265	255 245	226	206	177	157	137		
	WSt 355	 35	35 70	355 335	304 294	284 275	255	235	216	196	167		
	WSt 380	 35	35 70	375[1)] 345	333 324	314 304	284	265	245	216	186		
	WSt 420	 35	35 70	410[1)] 385	363 353	343 333	314	284	265	235	206		
	WSt 460	 35	35 70	450[1)] 420	402 392	373 363	343	314	294	265	235		
	WSt 500	 35	35 70	480[1)] 450	422 412	392 382	363	333	314	284	255		
Baustähle DIN 17100	**St 37-2, St 37-3** USt 37-2 RSt 37-2	 16 40	16 40 65	235 225 215	218 208 200	202 192 185	185 175 170	165 155 150	140 135 130				
	St 44-2	 16 40	16 40 65	275 265 255	248 245 237	232 225 218	215 205 200	195 185 180	165 160 155				
	St 52-3	 16 40	16 40 65	355 345 335	318 308 300	282 272 265	245 235 230	225 215 210	195 190 185				

[1)] bis 16 mm Dicke um ca. 10 N/mm^2 höher.

Mindestwanddicke von zylindrischen Mänteln mit $D_a/D_i \leqq 1{,}2$ bei Druckbehältern bzw. 1,7 bei Dampfkesseln sowie von Rohren mit $d_a \leqq 200$ mm und $d_a/d_i \leqq 1{,}7$

$$s = \frac{D_a \cdot p}{2\frac{K}{S}v + p} + c = \frac{D_i \cdot p}{2\frac{K}{S}v - p} + c \leqq s_e \qquad (4.18)$$

s	in mm	erforderliche Mindestwanddicke,
s_e	in mm	ausgeführte Wanddicke,
D_a, D_i	in mm	Außen- bzw. Innendurchmesser des zylindrischen bzw. kugeligen Mantels oder gewölbten Bodens, bei Rohren = d_a bzw. d_i,
p	in N/mm²	Berechnungsdruck = höchstzulässiger Betriebsüberdruck (1 N/mm² = 1 MPa = 10 bar oder 1 bar = 0,1 N/mm²),
β		Berechnungsbeiwert für gewölbte Böden nach Tab. 4.23, für kugelige Mäntel und Halbkugelböden ist $\beta = 1$,
K	in N/mm²	Festigkeitskennwert des Werkstoffs nach den Tabn. A 4.24 und A 4.25,
S		Sicherheitsbeiwert nach Tab. A 4.26,
v		Schweißnahtfaktor, der die Wertigkeit der Schweißnaht gegenüber dem Blech berücksichtigt, in der Regel = 0,8. Höherbewertung bis $v = 1$ nach vorausgegangenen Prüfungen. Bei ungeschweißten Teilen und bei äußerem Überdruck ist $v = 1$,
c	in mm	Wanddickenzuschlag nach Tab. A 4.26.

[2] Extract from the Standard EN 13445

5.2.3 Relation entre les définitions relatives à l'épaisseur

Les relations entre les différentes définitions relatives à l'épaisseur sont illustrées Figure 5-1.

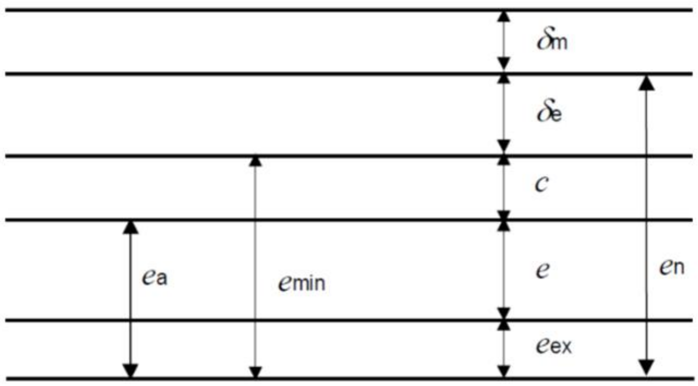

Légende

e est l'épaisseur requise

e_n est l'épaisseur nominale

e_{min} est l'épaisseur minimale possible après fabrication ($e_{min} = e_n - \delta_e$)

e_a est l'épaisseur utile ($e_a = e_{min} - c$)

c est la surépaisseur de corrosion ou d'érosion

δ_e est la valeur absolue de la tolérance négative éventuelle relative à l'épaisseur nominale (prise dans les normes de matériaux par exemple)

δ_m est la surépaisseur relative à l'amincissement possible pendant la fabrication

e_{ex} est l'épaisseur complémentaire pour atteindre l'épaisseur nominale

[3]-https://www.techniques-ingenieur.fr/base-documentaire/mecanique-th7/stockage-et-transfert-des-fluides-des-machines-hydrauliques-et-thermiques-42174210/tuyauteries-resistance-des-elements-bm6720/dimensionnement-calcul-de-resistance-a-la-pression-bm6720niv10003.html#niv-sl3974465

Les contraintes directes sont régies par les mêmes formules que la pression intérieure (figure **2**). La tension de compression maximale se produit à la face interne et vaut :

$$\sigma_{ti} = \frac{2p_e R_e^2}{R_e^2 - R_i^2} \qquad (8)$$

Pour les tubes minces, il suffit d'inverser le signe de la pression et l'on calcule :

$$\boxed{\sigma_t = \frac{-p_e R_m}{a}}$$

et

$$\boxed{\sigma_\ell = \frac{-p_e R_m}{2a}}$$

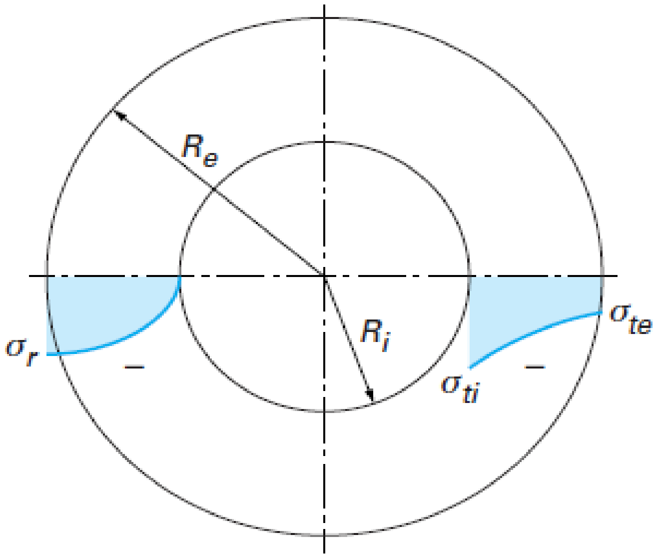

[4] CODAP 2005 Division 2, Partie C-Conception et Calculs

Caractéristique matériau		
Type	316L	1.4404
Rp 0.2	220	[MPa]
Rp 1.0		[MPa]
Re		[MPa]
Rm	520	[MPa]
Technical Pocket Guide (Schaffler)		

Contrainte nominale de calcul			
Rp 1.0 / 1.2	183.3	[MPa]	Calcul
Rm / 3	173.3	[MPa]	
f	173.3	[MPa]	
f	25	[ksi]	ASME
	172.37	[MPa]	
Zone locale (interne)	63.25	[mm]	
Zone locale (externe)	54.8	[mm]	

Zones		
Contrainte maximale générale de membrane	172.4	[MPa]
Contrainte minimale pour un zone locale	189.6	[MPa]
Contrainte maximale locale de membrane	258.6	[MPa]

[5] https://engstandards.lanl.gov/esm/pressure_safety/process_piping_guide_R2.pdf

12 Prototype one: excel data and result

Données			
Données tube			
Rayon extérieur	R_e	16.7	[mm]
Rayon intérieur	Ri	12.7	[mm]
Rayon moyen	R_m	14.7	[mm]
Épaisseur de paroi	s_e	4	[mm]
Section	S_{feet}	369.5	[mm^2]
Moment quadratique	I_y	40656.3	[mm^4]
Nombre de pieds	n	4	[-]
Données matériau			
Module élastique	E	210	[GPa]
Module de Poisson	v	0.3	[-]
Limite élastique	F_e	207	[MPa]
Charge			
Masse réservoir	m_{res}	664	[kg]
Masse eau	m_{eau}	1000	[kg]
Accélération gravitationnelle	g	9.81	[m/s^2]
Poids	F_g	16323.8	[N]

Calculs			
Compression			
Contrainte	σ_{feet}	11.05	[MPa]
Flambage			
Longueur maximale d'un pied	l	170	[mm]
Longueur de flambage	l_k	119	[mm]
Force limite de flambage	F_k	5865.5	[N]
Poids par pied	$F_{g,1}$	4080.96	[N]

13 Prototype two: excel data and result

Données			
Données pieds			
Côtés externes	x_{e1}	80	[mm]
	x_{e2}	50	[mm]
Côtés internes	x_{i1}	76	[mm]
	x_{i2}	46	[mm]
Section	S_{feet}	504.0	[mm^2]
Moment quadratique	I_y	450592.0	[mm^4]
	I_y	216872.0	[mm^4]
	I_y	216872.0	[mm^4]
Nombre de pieds	n	4	[-]
Données matériau			
Module élastique	E	210	[GPa]
Module de Poisson	v	0.3	[-]
Limite élastique	F_e	207	[MPa]
Charge			
Masse réservoir	m_{res}	664	[kg]
Masse eau	m_{eau}	1000	[kg]
Accélération gravitationnelle	g	9.81	[m/s^2]
Poids	F_g	16323.8	[N]

Calculs			
Compression			
Contrainte	σ_{feet}	8.10	[MPa]
Flambage			
Longueur maximale d'un pied	l	450	[mm]
Longueur de flambage	l_k	315	[mm]
Force limite de flambage	F_k	4465.3	[N]
Poids par pied	$F_{g,1}$	4080.96	[N]

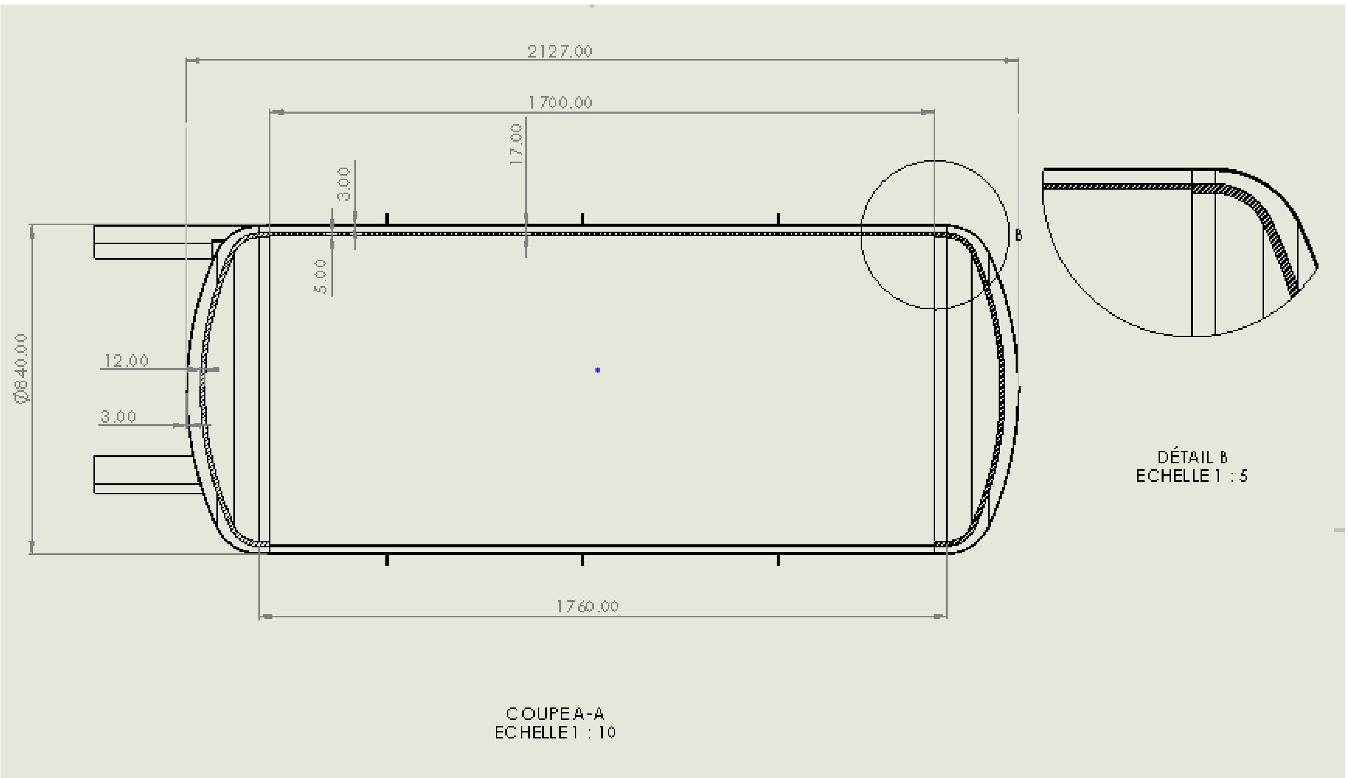
2127.00
1700.00
17.00
3.00
5.00
B
12.00
3.00
Ø840.00
1760.00
DÉTAIL B
ECHELLE 1 : 5
COUPE A-A
ECHELLE 1 : 10